

Review

Enhanced Heat Transfer Using Oil-Based Nanofluid Flow through Conduits: A Review

Sunil Kumar ¹, Mridul Sharma ¹, Anju Bala ¹, Anil Kumar ^{2,*}, Rajesh Maithani ^{2,*} , Sachin Sharma ² ,
Tabish Alam ^{3,*} , Naveen Kumar Gupta ⁴ and Mohsen Sharifpur ^{5,6} 

¹ Yogananda School of AI, Computer and Data Sciences, Shoolini University, Solan 173229, India

² Mechanical Engineering Department, University of Petroleum and Energy Studies, Dehradun 248007, India

³ CSIR-Central Building Research Institute, Roorkee 247667, India

⁴ Mechanical Engineering Department, Institute of Engineering and Technology, GLA University, Mathura 281406, India

⁵ Nanofluids Research Laboratory, Department of Mechanical and Aeronautical Engineering, University of Pretoria, Pretoria 0002, South Africa

⁶ Department of Medical Research, China Medical University Hospital, China Medical University, Taichung 404, Taiwan

* Correspondence: k.anil@ddn.upes.ac.in (A.K.); rmaithani@ddn.upes.ac.in (R.M.); tabish.iitr@gmail.com (T.A.)

Abstract: The application of nanofluids for enhancing the heat transfer rate is widely used in various heat exchanger applications. The selection of oil as the base to prepare nanofluids significantly enhances the thermal performance, due to its high heat carrying capacity as compared to conventional base fluid. A review is performed of various heat exchanger conduits having base fluid as nanoparticles with oil. It is reported that the heat transfer rate of a heat exchanger is significantly increased with the use of oil-based nanofluids. The rate of heat transfer depends on the type of nanoparticle, its concentration and diameter, the base fluid, as well as factors like the mixture of more than two nanoparticles (hybrid nanofluids) and stability. A review is also performed of the thermal performance of the different nanofluids analyzed by various investigators. The heat transfer system reviewed in this work includes triangular, square, and circular conduits, as well as rib surface conduits. The review of various applications viz. solar thermal systems, heat exchangers, refrigerators, and engines, is carried out where the inclusion of the oil base is used. It is reported that the amalgamation of the nanomaterial with the oil as base fluid is a prolific technique to enhance thermal performance. The performance of the reviewed research work is comparatively analyzed for different aspects viz. thermal oil, mineral oil, hybrid, and conventional nanoparticles, concentration of nanoparticles, etc. The novelty of the present work is the determination of the effective performing oil-based nanofluid in various applications, to figure out the selection of specific mineral oil, thermal oil, nanoparticle concentration, and hybrid nanofluids.

Keywords: nanofluids; heat transfer; thermal conductivity; volume fraction; oil-based



Citation: Kumar, S.; Sharma, M.; Bala, A.; Kumar, A.; Maithani, R.; Sharma, S.; Alam, T.; Gupta, N.K.; Sharifpur, M. Enhanced Heat Transfer Using Oil-Based Nanofluid Flow through Conduits: A Review. *Energies* **2022**, *15*, 8422. <https://doi.org/10.3390/en15228422>

Academic Editor: Marco Milanese

Received: 29 September 2022

Accepted: 5 November 2022

Published: 10 November 2022

Publisher's Note: MDPI stays neutral with regard to jurisdictional claims in published maps and institutional affiliations.



Copyright: © 2022 by the authors. Licensee MDPI, Basel, Switzerland. This article is an open access article distributed under the terms and conditions of the Creative Commons Attribution (CC BY) license (<https://creativecommons.org/licenses/by/4.0/>).

1. Introduction

The consumption of energy in an effective manner is a major challenge and can be achieved by using source energy more efficiently or by reducing the magnitude of the facility used. Developing a heat exchanger of high efficiency, which is lightweight, low in cost, and of a compact size leads to the investigation of heat transfer enhancement techniques [1]. The environmental considerations and energy cost encourage modification of the existing designs for enhanced performance in chemical engineering, air conditioning, electronic chip cooling, power systems, and aerospace applications. Heat transfer rate between the hot surface and fluid can be enhanced by various methodologies, such as increasing the heat transferring area that augments heat transfer coefficient (HTC). The

incorporation of micrometer-sized metal powders to heat-transferring fluids enhances the thermal conductivity of fluids [2].

Industrial applications benefit from enhanced heat transfer fluids, and the nanofluids have the potential to bring down thermal resistances. The suspended nanoparticles have higher thermal conductivities as compared to the base fluids (water, ethylene glycol, etc.) and a higher rate of heat transfer is seen using the nanofluids, even at low volume concentrations. The addition of nanoparticles to a base fluid in a heat exchanger considerably enhances the rate of convective heat transfer [3]. The viscosity determines the flow capabilities and driving force, i.e., pumping power for the transport of the fluid.

The objective of the present work is to comparatively analyze the performance of the oil-based nanofluid reviewed to reach a conclusion defining the best suited oil-based nanofluid for a specific application. The review of various applications such as heat exchangers, solar thermal systems, refrigerators, and engines is performed using oil as a base fluid. The secondary objective is to compare the performance of literature reviewed for different thermal oil, mineral oil, hybrid and conventional nanoparticles, and the concentration of nanoparticles used in a specific application. This comparison will determine the best performing selected oil-based nanofluid for various applications.

2. Nanofluids: Preparation and Stabilization

Nanofluids are fluids made by suspending nanoparticles in base fluids. Nanoparticles are different from micro- or macro-sized materials. We should be concerned about the possible detrimental impact of nanoparticles on humans or the environment, since it is unknown if nanoparticles of certain materials and sizes might harm the environment and health [4]. As for their low heat transfer qualities, common heat transfer fluids such as water, ethylene glycol, and motor oil have limited heat exchange capabilities. Metals' thermal conductivities are approximately three times greater than fluids. Therefore, it makes sense to mix the two to create a thermal performance medium that behaves like a fluid but has the thermal properties of a metal. A nanofluid is a two-phase combination with nanosized particles in the solid phase [5]. Many experiments have been conducted to improve heat transmission utilizing nanofluids. Nanoparticles suspended in a fluid improve perceived thermal conductivity while also changing viscosity and density [6].

Nanofluids modeling may be done in two ways: single and two phases. Researchers have considered nanofluids as normal pure fluids in a single step and employed standard mass, momentum, and energy equations. Researchers assumed slip velocities between nanoparticles and fluid molecules in the first phase [7,8].

Preparation of Nanofluids

The preparation of the nanofluid is a critical stage in determining the stability of the nanofluid. The chemical inertness and strength and durability of suspended nanoparticles are required to use nanofluids in practical uses. Even suspension, ensuring appropriate, durable suspension, no chemical reactions in the type of combination, the dispersion medium, thermal stability, chemical compatibility, and preparation processes are desired characteristics for manufacturing nanofluids. There seem to be two major approaches for preparing nanofluids: one-step and two-step, or dispersion processes [9].

One technique is conducted by producing nanofluids through evaporation of a nanoparticle source and deposition of evaporating into a base fluid. The base fluid, including oil or ethylene glycol, is put in a cylindrical drum with a thermal and exchanger-cooler device that can be adjusted. As the drum rotates, a thin liquid layer forms inside the drum. An insulated heater-boat-evaporator and heat exchanger cooler device.

A thin liquid layer forms on the interior surface of the drum as it circles. As an insulated heating element with a melting material located within its boat evaporator, the evaporated substance is warmed, evaporating a portion of the evaporation material and creating nanoparticles; the nanoparticles are absorbed by the liquid film to produce nanofluid [10].

The most common method is the two-step method. Powder nanoparticles manufactured or purchased are used in the dispersion process. The nanoparticles are dispersed into the base fluids using ultrasonic agitation, mechanical stirring, the addition of a dispersant or a pH-5.0 nanofluid. The clumps of nanoparticles are broken down by mechanical churning and ultrasonic stirring to prevent the re-aggregation of nanoparticles and produce stable nanofluids, add dispersion or modify pH. The two-step procedure typically begins with the creation of nanoparticles by a physical or chemical process (such as evaporation and inert-gas condensation processing) before breaking them up into a base fluid [10].

3. Governing Equation and Correlation Used to Calculate Thermo Physical Properties of Nanofluids

Nanofluids have a wide range of properties, but their key characteristics are their thermal conductivity, density, specific heat, and viscosity. These characteristics include the particle size, heat, chemical composition, and interfacial characteristics at the particulate interface, in addition to the volume fraction of particles and particle-fluid conductivity ratio [11].

3.1. Thermal Conductivity

The characteristic that has attracted the most interest from the research community is thermal conductivity. In terms of temperature change, thermal conductivity is defined as the amount of heat given per unit of time and per unit of surface area divided by watts per degree Kelvin. When suspending metal or non-metal, the heating rate is a crucial thermal characteristic for increasing the heat transfer of liquids. To create the regression equation, various data points on the thermal conductivity of metallic and metal oxide nanofluids, such as Al_2O_3 , Fe_3O_4 , TiO_2 , ZnO , ZrO_2 , and CuO are accessible via the literature [12].

Since the heat capacity of these fluids significantly impacts the temperature transfer between the heat transfer medium and the heat transfer surface, conventional heat transfer fluids like oil, water, and mixtures of ethylene glycol are poor heat transfer fluids. Therefore, various techniques have been used to increase the thermal conductivity of these fluids by suspending materials in liquids made up of nano/micro- or larger-sized particles [13]. The various thermal conductivity equations from numerous authors are included in Table 1.

Table 1. Equations used for calculating the thermal conductivity of nanofluids.

Investigators	Equations
Navaei et al. [14]	$k_{\text{eff}} = k_{\text{static}} + k_{\text{brownian}}$ $k_{\text{static}} = k_f \frac{[(k_{\text{np}} + 2k_f) - 2\phi(k_f - k_{\text{np}})]}{[(k_{\text{np}} + 2k_f) + \phi(k_f + k_{\text{np}})]}$ $k_{\text{brownian}} = 5 \times 10^4 \beta \phi \rho_p C_p f \sqrt{\frac{kT}{2\rho_{\text{np}} R_{\text{np}}}} f(T, \phi)$
Ahmad et al. [12]	$\frac{k_{\text{eff}}}{k_f} = \frac{k_p + 2k_f - 2\phi(k_f - k_p)}{k_p + 2k_f + \phi(k_f - k_p)}$
Haridas et al. [15]	$k_{\text{nf}} = k_w \left[0.8938 \left(1 + \frac{\phi}{100} \right)^{1.37} \left(1 + \frac{t_f}{70} \right)^{0.2777} \left(1 - \frac{\rho_w}{150} \right)^{-0.0366} \left(1 - \frac{\alpha_w}{\alpha_w} \right)^{0.01737} \right]$
Dogonchi et al. [16]	$\frac{k_{\text{nf}}}{k_f} = \frac{k_s + 2k_f - 2\phi(k_f - k_s)}{k_s + 2k_f + 2\phi(k_f - k_s)}$
Yang et al. [17]	$k_{\text{nf}} = \frac{k_p + 2k_{\text{bf}} - 2(k_{\text{bf}} - k_p)\phi}{k_p + 2k_{\text{bf}} + (k_{\text{bf}} - k_p)\phi} k_{\text{bf}} + \epsilon \beta \rho_{\text{bf}} C_{p,\text{bf}} \sqrt{\frac{kT}{\rho_p d_p}} f(T, \phi)$

3.2. Density

Mass per unit volume is the definition of density. It may be measured in kilograms per liter and grams per milliliter. For estimating the density of nanofluids, several researchers have developed various equations using various relationships. Table 2 lists a few of them.

Table 2. Equations used for calculating the density of nanofluids.

Investigators	Equations
Kumar et al. [9]	$\rho_{nf} = (1 - \phi)\rho_{bf} + \phi\rho_{nf}$
Hussein et al. [18]	$\rho_{nf} = \left(\frac{\phi}{100}\right)\rho_p + \left(1 - \frac{\phi}{100}\right)\rho_f$
Ahmad et al. [19]	$\rho_{nf} = (1 - \phi)\rho_f + \phi\rho_p$
Dogonchi et al. [16]	$\rho_{nf} = (1 - \phi)\rho_{bf} + \phi\rho_s$

3.3. Specific Heat Capacity

The quantity of heat a substance requires to cause temperature change is referred to as its specific heat capacity. The specific heat is increased because the surface atoms of the nanoparticles have a larger specific surface energy than the bulk material. Additional thermal storage mechanisms induced by interfacial interactions between nanoparticles and liquid molecules may contribute to the increase in particular heat [20]. The nanoparticle's large specific interfacial area may absorb liquid molecules to its surface and create liquid layers, which reversely constrains the nanoparticle and converts its free boundary surface atoms to non-free inner atoms. This impact will increase the specific heat capacity of the nanofluid even more [18]. Many scientists have provided additional heat capacitance formulae, which are included in Table 3.

Table 3. Equations used for calculating the specific heat capacity of nanofluids.

Investigators	Equations
Kumar et al. [9]	$C_{Pnf} = \frac{\phi\rho_{np}C_{Pnf} + (1-\phi)\rho_{bf}C_{bf}}{\rho_{nf}}$
Ahmad et al. [12]	$(\rho C_p)_{nf} = (1 - \phi)(\rho C_p)_f + \phi(\rho C_p)_s$
Dogonchi et al. [16]	$(C_p\rho)_{nf} = (1 - \phi)\rho_{bf}C_{p,bf} + \phi\rho_s C_{p,s}$
Yang et al. [17]	$C_{pnf} = \frac{((1-\phi)_p\rho C_p)_{bf} + \phi(\rho C_p)_p}{\rho_{nf}}$
Vanakiet al. [18]	$(C_p)_m = \frac{((1-\phi_p) \times \rho_f \times (C_p)_f) + \phi_p \times (\rho_p \times C_p)_p}{\rho_m}$

3.4. Viscosity

Viscosity is defined as friction among fluid particles. It may measure viscosity using a viscometer, which is a piece of equipment that regulates the amount of force required to move through a liquid. Another parameter that influences the Nusselt number and flow friction is viscosity [21]. Several authors have employed computational and experimental research using various formulae to estimate the viscosity of nanofluids. Table 4 shows a selection of them.

Table 4. Equations used for calculating the viscosity of nanofluids.

Investigators	Equations
Kumar et al. [9]	$\mu_{nf} = \mu_b (123\phi^2 + 7.3\phi + 1)$
Navaei et al. [14]	$\mu_{nf} = \frac{\mu_f}{(1-\phi)^{2.5}}$
Ahmad et al. [12]	$\mu_{eff} = \mu_f \frac{1}{1 - 34.87(dp/df)^{-0.3} \times \phi^{1.03}}$
Yang et al. [17]	$\frac{\mu_{nf}}{\mu_{bf}} = 123\phi^2 + 7.3\phi + 1$

Their thermo-physical characteristics determine nanofluids' heat transmission behavior. Conventional heat transfer fluids such as water, oil, propylene glycol, and others have

naturally modest heat transfer rates, making them inappropriate for applications requiring high heat transfer rates [19]. Thermophysical properties and parameters such as the Reynolds number (Re), the Prandtl number (Pr), volume concentration (φ) of nanoparticles affecting heat transfer (Nu), and flow friction (ff) of fluids. Ho et al. [22] proposed Nu relations for four distinct models based on two formulae for $0\% \leq \varphi \leq 4\%$. The findings revealed that the uncertainties associated with the formulas used significantly influenced heat transfer characteristics.

Correlation formulations for Nu and ff offered by researchers such as Petukhov [23]; Gnielinski [24]; Dittus and Boelter [25]; Maiga and Bécaye [26]; Duangthongsuk and Wongwises [27]; Suresh et al. [28]; Sundar et al. [29]; and Madhesh et al. [30] are listed in Table 5.

Table 5. Correlation relations for Nusselt number and flow friction for various flow regimes.

Researchers	Correlations
Petukhov [23]	$\text{Nu} = \frac{\text{RePr}(f/8)}{1.07+12.7(f/8)^{0.5}(\text{Pr}^{0.66}-1)}$ $f = (1.82 \log \text{Re} - 1.64)^{-2}$
Gnielinski [24]	$\text{Nu} = \frac{(f/8)(\text{Re}-1000)\text{Pr}}{1+12.7(f/8)^{0.5}(\text{Pr}^{0.66}-1)}$ $f = 0.079\text{Re}^{-1/4}$
Dittus and Boelter [25]	$\text{Nu} = \begin{cases} 0.024\text{Re}^{0.8}\text{Pr}^{0.4} & \text{for heating} \\ 0.024\text{Re}^{0.8}\text{Pr}^{0.3} & \text{for cooling} \end{cases}$
Maiga and Bécaye [26]	$\text{Nu} = 0.085\text{Re}^{0.71}\text{Pr}^{0.35}$
Duangthongsuk and Wongwises [27]	$\text{Nu} = 0.074\text{Re}^{0.707}\text{Pr}^{0.385}\varphi^{0.074}$
Suresh et al. [28]	$\text{Nu} = 0.31(\text{RePr})^{0.68}(1+\varphi)^{95.73}$ $f = 26.44\text{Re}^{-0.8737}(1+\varphi)^{156.23}$
Sundar et al. [29]	$\text{Nu} = 0.215\text{Re}^{0.8}\text{Pr}^{0.5}(1+\varphi)^{0.78}$ $f = 0.3108\text{Re}^{-0.245}(1+\varphi)^{0.42}$
Madhesh et al. [30]	$\text{Nu} = 0.012\text{Re.Pr}^{0.333}(\varphi)^{0.032}$

4. Investigations of Heat Transfer Characteristics of Oil-Based Nanofluids for Varying Particle Concentration in Various Applications

The utilization of the Oil-Based Nanofluids finds its application in various applications as shown in Figure 1. Various applications using the oil-based nanofluids delivers an effective and prolific results in their performance. Hwang et al. [31] reported augmentation in the thermal conductivity of nanofluids with an increase in the particle volume fraction (φ); except for nanofluids with water as base of low thermal conductivity. Hekmatipur et al. [32] and Javed et al. [33] synthesized a copper oxide nanofluid and found that the thermal properties increased as compared to the base fluid. The nanoparticles such as copper oxide, fullerene, silicon dioxide, and multi-walled carbon nanotubes (MWCNT) with base fluids (water, ethylene glycol, etc.) were studied by Hwang et al. [34], Vasheghani et al. [35], Yu et al. [36], Gholamipour et al. [37], and Farbod et al. [38]; the studies reported that increasing the value of φ enhances the thermal conductivity of nanofluids.

Oil Based Nanofluids- Composition and Application		
Type of oil	Nanoparticle used	Application
<ul style="list-style-type: none"> • Thermal Oil • Crude oil • Vegetable Oil • Pure oil • Palm Oil • Engine Oil • Mineral Based oil 	<ul style="list-style-type: none"> • Carbon nano tubes (CNT) • Copper Oxide • Fullerene • Silicon dioxide • Multi-walled carbon nanotubes (MWCNT) • Titanium dioxide • Aluminum dioxide • Iron Oxides 	<ul style="list-style-type: none"> • Heat Exchangers • Solar thermal Collectors • Refrigerators • Engines • Grinding

Figure 1. Nanofluid applications.

Xue ZQ [39] and Sauvad [40] found that HTC, using a $\text{TiO}_2\text{-SiO}_2$ nanofluid, is boosted by elevating the temperature and concentration volume. The maximum augmentation in the heat transfer rate is reported to be 81%, as compared to the base fluid for a selected concentration volume and temperature of 3.0% and 70 °C, respectively.

Sundar et al. [41] and Rahimi et al. [42] analyzed nanofluids by dissolving synthesized nanoparticles of $\text{GO}/\text{Co}_3\text{O}_4$ with water and ethylene glycol, and reported an increase in thermal conductivity of water-based nanofluids by 19.14% and an increase in ethylene glycol-based nanofluids by 11.85% at $\phi = 0.2\%$. Aberomand [43] conducted a study on oil-based nanofluids, including silver nanoparticles, and observed that thermal conductivity is temperature dependent in the range of 40 to 100 °C at various weight fractions from 0.12% to 0.72%. Salimi et al. [44] showed that, by increasing the Reynolds number (Re) from 300 to 900, the rate of heat transfer is enhanced by 9.5%. Sokhansefat et al. [45] numerically studied Al_2O_3 nanoparticles in synthetic oil for enhancement in heat transfer rate. The numerical analysis revealed that the convective HTC is directly affected by the volumetric concentration of the nanoparticles. Carvalho and Fossum [37] reported an escalation in the thermal conductivity of nanofluids by increasing the weight percentage of the nanoparticles. The highest Nusselt number (Nu) ratios for a Re of about 800 were found to be 1.15, 1.31, and 38 for $\text{Al}_2\text{O}_3/\text{turbine oil}$ (0.50%), $\text{TiO}_2/\text{turbine oil}$ (0.50%), and $\text{CuO}/\text{turbine oil}$ (0.50%), respectively.

Sidik et al. [46,47] reported higher heat transfer rates using hybrid nanofluids as compared to commonly used heat transfer fluids, such as water, ethylene glycol, and oil. Kumar and Gaurav [48] and Hemmat et al. [49] found that nanoparticle suspension required lower specific energy for grinding as compared to sunflower oil. Amiri et al. [50], Aghaei et al. [51], and Ilyas et al. [52,53] found that viscosity increased when the nanoparticle volume fraction was increased, and decreased when temperature was increased. The use of a nanofluid-based technique could save fuel in the oil industry and solve issues brought about by limited access to a diluent [54–56]. Table 6 represents the optimum parameters and major findings of oil-based nanofluids in previous investigations.

Table 6. Optimum parameters and major findings of oil-based nanofluids in previous investigations.

Author's Name	Nanoparticle	Parameter	Optimum Parameter	Remarks
Manoj and Ghosh [2]	MWCNT	$\varphi = 0.6 - 1.4\%$ $d_{np} = 50 \text{ nm}$	$\varphi = 1\%$	The Nu for MWCNT nanofluid is 35% higher than that of soluble oil.
Farbod et al. [38]	Cu_5Zn_8	$\varphi = 0.2 - 3\%$ $d_{np} = 21 \text{ nm}$	$\varphi = 1\%$	The sintering of Cu_5Zn_8 nanoparticles showed a small change in the thermal conductivity of nanofluid.
Sauvad [40]	TiO_2 , SiO_2	$\varphi = 0.5 - 3.0\%$ $d_{np} = 50 \text{ nm}$ $T = 30, 50, 70 \text{ }^\circ\text{C}$ $\text{Re} = 3000 - 18,000$	$\varphi = 3.0\%$ $T = 70 \text{ }^\circ\text{C}$ $\text{Re} = 18,000$	The Nu of SiO_2 nanofluid is higher than TiO_2 nanofluid. The maximum enhancement Nu is found to be 81% at $\varphi = 3\%$.
Sundar et al. [41]	Co_3O_4	$\varphi = 0.05\% - 0.2\%$ $T = 20 - 60 \text{ }^\circ\text{C}$	$\varphi = 0.2\%$ $T = 60 \text{ }^\circ\text{C}$	The viscosity enhancement of water-based nanofluid is 1.70 times, and ethylene glycol based nanofluid is 1.42 times at $\varphi = 0.2\%$ and $T = 60 \text{ }^\circ\text{C}$.
Rahimi et al. [42]	DWCNT	$\varphi = 0.01 - 0.5\%$ $T = 20 - 50 \text{ }^\circ\text{C}$	$\varphi = 0.05\%$ $T = 50 \text{ }^\circ\text{C}$	The optimum value of solid volume fraction for highest value of average HTC and Nusselt number is 0.05 vol%.
JA Aberomand [43]	Cu	$\varphi = 0.12 - 0.72\%$ $d_{np} = 20 \text{ nm}$ $\text{Re} = 0 - 140$	$\varphi = 0.72$ $\text{Re} = 140$	Finned annular tube can improve this enhancement by about 33% compared to the base fluid.
Salimi et al. [44]	TiO_2	$\varphi = 0.3 - 1\%$ $\text{Re} = 300 - 900$ $d_{np} = 20 \text{ nm}$	$\varphi = 1\%$ $\text{Re} = 900$	The Soluble oil-based TiO_2 nanofluid improved heat transfer rate due to its promising thermal and lubricating properties.
Sokhansefat et al. [45]	Al_2O_3	$\varphi = 0 - 5\%$ $d_{np} = 70 \text{ nm}$ $T = 300 - 500 \text{ }^\circ\text{C}$	$\varphi = 5\%$ $T = 500 \text{ }^\circ\text{C}$	The Nu is increased as the φ of the nanoparticles in the base fluid is increased.
Ilyas et al. [52]	Al_2O_3	$\varphi = 0.5 - 3\%$ $d_{np} = 40 \text{ nm}$ $T = 25 - 90 \text{ }^\circ\text{C}$	$\varphi = 3\%$ $T = 25 \text{ }^\circ\text{C}$	Effective thermal conductivity of nanofluids is improved as compared to pure oil.
Zareh and Davoodi [57]	CuO SiO_2	$\varphi = 0.3 - 1.0\%$ $d_{np} = 20 - 70 \text{ nm}$	$\varphi = 0.7\%$	Both CuO and SiO_2 NPs are capable of enhancing the friction reduction ability of vegetable oils 21–31%, respectively.
Qin et al. [58]	CuS	$\varphi = 0.01 - 0.04 \%$ $d_{np} = 60 \text{ nm}$ $T = 30 - 60 \text{ }^\circ\text{C}$	$\varphi = 0.04\%$ $T = 30 \text{ }^\circ\text{C}$	The thermal conductivity of nanofluids increased with an increased volume fraction and obtained Nu enhancement up to 20.5% for a volume fraction of 0.04% at 30°C.

Table 6. Cont.

Author's Name	Nanoparticle	Parameter	Optimum Parameter	Remarks
Zheng et al. [59]	SiO ₂	$\varphi = 0.5\text{--}2.0\%$ $T = 0\text{--}90\text{ }^\circ\text{C}$	$\varphi = 2.0\%$ $T = 80\text{ }^\circ\text{C}$	The viscosity of solution increased with addition of nano- SiO ₂ (0.5–2.0 wt%).
Tabari and Heris [60]	MWCNT	$\varphi = 0.25\text{--}0.55\%$ $d_{\text{np}} = 15\text{ nm}$	$\varphi = 0.55\%$	HTC and Nu of pure water increased by adding MWCNT.
Razi et al. [61]	CuO	$\varphi = 0.2\text{--}2.0\%$ $d_{\text{np}} = 50\text{ nm}$ $Re = 10\text{--}100$	$\varphi = 2.0\%$ $Re = 100$	Nanofluid have better Nu when they flow in flattened tubes rather than in round tubes. Maximum enhancement in Nu of 16.8%, and 26.4% is obtained for nanofluid flow with 2% wt. concentration inside the round tube and flattened tubes
Moraveji and Hejazian [62]	CuO	$\varphi = 0.1\text{--}2\%$ $Re = 10\text{--}90$ $d_{\text{np}} = 50\text{ nm}$	$\varphi = 2\%$ $Re = 85$	The Nu for nanofluid is 28% larger than the base fluid; pressure drop in helical tube is approximately three times higher than the straight tube.
Heris et al. [63]	CuO, TiO ₂ , and Al ₂ O ₃	$\varphi = 0.1\text{--}0.5\%$ $Re = 350\text{--}850$ $d_{\text{np}} = 30\text{--}50\text{ nm}$	$\varphi = 0.50\%$ $Re = 850$	Adding CuO, TiO and Al ₂ O ₃ nanoparticles led to higher Nu as compared to the pure oil. The CuO/turbine oil nanofluid has better performance as compare to other NPs.
Ghazvini et al. [64]	Diamond	$\varphi = 0.2\% \text{--} 2.0\%$ $Re = 200\text{--}1000$	$\varphi = 2.0\%$ $Re = 1000$	Using engine oil-based nanofluid as the coolant in the plain tube: Nu enhances by about 60%.
Sundar et al. [65]	ND-Ni	$\varphi = 0.02\text{--}0.1\%$ $T = 24\text{--}65\text{ }^\circ\text{C}$ $d_{\text{np}} = 40\text{--}50\text{ nm}$	$\varphi = 0.1\%$ $T = 65\text{ }^\circ\text{C}$ $d_{\text{np}} = 40$	The electrical conductivities of both H ₂ O– and EG-based ND-Ni nanofluids are significantly greater than its base fluids. Furthermore, the electrical conductivity enhancement for H ₂ O–based ND-Ni nanofluid is higher compared to that of EG based ND-Ni nanofluid.
Ingole et al. [66]	TiO ₂	$\varphi = 0.25, 2\%$ $d_{\text{np}} = 20\text{--}25\text{ nm}$	$\varphi = 2\%$ $d_{\text{np}} = 20$	Addition of TiO ₂ nanoparticles reduced the variability and stabilized the frictional behavior.
Beheshti et al. [67]	MWCNT	$\varphi = 0.001, 0.01\%$ $d_{\text{np}} = 10\text{--}20\text{ nm}$ $T = 20\text{--}80\text{ }^\circ\text{C}$	$\varphi = 0.01\%$ $T = 80\text{ }^\circ\text{C}$	At all concentrations and temperatures, the viscosity of the nanofluid was lower than that of transformer oil.

Table 6. Cont.

Author's Name	Nanoparticle	Parameter	Optimum Parameter	Remarks
Arani et al. [68]	Ag-oil	$\varphi = 0.011 - 0.171\%$ $d_{np} = 20 \text{ nm}$	$\varphi = 0.171\%$	HTC increased by using nanofluid instead of pure oil. Maximum enhancement of HTC occurs in 0.171 vol%.
Wang et al. [69]	Al ₂ O ₃	$\varphi = 0 - 0.05\%$ $d_{np} = 28 \text{ nm}$	$\varphi = 0.05\%$	The collector efficiencies of the PTC system using Al ₂ O ₃ /synthetic oil nanofluid are higher under all working conditions.
Su et al. [70]	Graphite	$\varphi = 0.1, 0.5\%$ $d_{np} = 35 \text{ nm}$	$\varphi = 0.5\%$	Graphite oil-based nanofluid MQL reduced cutting force and temperature as compared to dry cutting and MQL with the corresponding base oil.
Derakhshan and Behabadi [71]	MWCNT	$\varphi = 0.05 - 0.2\%$ $d_{np} = 8 \text{ nm}$ Re = 10 – 100 T = 40 – 80 °C	$\varphi = 0.2\%$ Re = 100 T = 80 °C	The maximum enhancement of Nu due to presence of nanoparticles is about 22% and 18% for horizontal plain and microfin tubes, respectively.
Isfahani et al. [72]	Al ₂ O ₃ MWCNT	$\varphi = 0-1.0\%$ T = 25 – 50 °C	$\varphi = 1\%$ T = 25 °C	The viscosity of the hybrid nanofluid increases with increasing nano-additives concentration and decreasing temperature.
Aberouand et al. [73]	Ag	$\varphi = 0.12 - 0.72\%$ $d_{np} = 10 \text{ nm}$ T = 40 – 100 °C	$\varphi = 0.72\%$ T = 100 °C	Maximum enhancement of thermal conductivity was about 17% for the nanofluid with mass concentration of 0.72% at 100 °C.
Wang et al. [74]	Cu and diamond	$\varphi = 1 - 3\%$ $d_{np} = 2 - 8 \text{ nm}$	$\varphi = 3\%$	The employment of nanofluids as the cooling medium of piston cooling gallery is an effective method to reduce the heat loading of pistons.
Gholami et al. [75]	MWCNT	$\varphi = 0 - 4\%$ Re = 1–100 $d_{np} = 50 \text{ nm}$	$\varphi = 4\%$ Re = 100	The existence of ribs enhances the friction factor and Nusselt number, significantly.
Mechiri et al. [76]	Cu-Zn	$\varphi = 0.1\% - 0.5\%$ $d_{np} = 25 \text{ nm}$ T = 25 – 55 °C	$\varphi = 0.5\%$ T = 30 °C	Cu-Zn with 50:50 combination results in better enhancement in thermal conductivity due to the Brownian motion of the particles.
Asadi et al. [77]	Al ₂ O ₃ -MWCNT	$\varphi = 0.125-1.5\%$ T = 25 – 50 °C	$\varphi = 1.5\%$ T = 50 °C	Thermal conductivity and dynamic viscosity increased as the solid concentration increased.

5. Application-Based Investigation of Oil-Based Nanofluids

The present section discusses the use of oil-based nanofluid in specific applications and the effect of using the discrete nanofluid as compared to the conventional one.

5.1. Investigation on Enhanced Oil Recovery Using Oil Based Nanofluids

Zheng et al. [59], Suleimanov et al. [78], Radnia et al. [79], Kuang et al. [80], and Emadi et al. [81] experimentally studied non-ferrous metal nanofluid in an aqueous solution of anionic surface-active agents and the addition of light, for enhanced oil recovery (EOR). It was revealed that the use of nanofluid reduces the surface tension on an oil boundary by 70% to 90% compared to the surface-active agent aqueous solution that results in a considerable EOR.

Hemmat et al. [82], Dai et al. [83], Liang et al. [84], and Chen et al. [85] concluded that surfactants could modify rock wettability and bring down the oil-water interfacial tension (IFT). Alnarabiji et al. [86] and Anssari et al. [87] reported that the efficiency of diluted nanofluids is enhanced by nanofluid concentration and immersion time. The results revealed new nanofluid potential to be used for improved EOR and efficient CO₂ geostorage. Zabala et al. [88] and Shahrabadi et al. [89] concluded that nanoparticles are promising agents and have more potential for EOR. The oil-based nanofluid also tripled in performance compared to conventional nanofluids. Hendraningrat and Torsæter [90], Zhao and Li [91], Youssif et al. [92], Bhunia [93], Valantina [94], and Gbadamosi et al. [95] investigated hydrophilic metal oxide particles with brine to determine the potential for EOR. They concluded that the presence of nanoparticles and dispersant reduced the IFT to yield significant EOR. Fontes et al. [96] and Khademolhosseini et al. [97] concluded that nanoparticles and bioproducts have an effect on each other. Because of a reduction in the IFT, an improvement of about 58% was obtained in mobility ratio and oil recovery.

Murshed et al. [98] analyzed the applicability of nanofluid and temperature effects on the surface tension, IFT, and viscosity for droplet-based microfluidics. A lower surface tension was reported with oil-based IFT as compared to base fluid. Mohammadi et al. [99] and Hussein et al. [100] analyzed nanoparticles in the solution and reported wetting alteration from oil-wet to strongly water-wet conditions, and also decreased the residual oil saturation and EOR by about 15%. Liu et al. [101] examined the mechanical properties of hybrid nanomaterials of nano-silica and graphene oxide of oil-well cement. The strength of cement for 1.5% nano-silica and 0.03% graphene oxide was increased by 43.2% and 42%, respectively, with 28 days of curing.

5.2. Investigation on Heat Exchanger Tube/Channel Using Oil-Based Nanofluids

Qi et al. [102] analyzed the TiO₂-water nanofluid for heat transfer rate and flow characteristics using triangular and circular tubes in the heat exchanger, and found that the nanofluid in a triangular tube enhances heat transfer more than in a circular tube. Lee et al. [103] studied the CuO/base oil nanofluid to determine the thermohydraulic properties in a smooth tube by using different wire coil inserts. Results show a 45% increase in HTC and a 63% enhancement in friction losses at a maximum Re. Razi et al. [104] found that the HTC and friction losses are increased by the use of nanofluids, and that the use of flattened tubes instead of round tubes enhances the convective HTC.

Ariana et al. [105] inspected heat transfer using turbine oil-based nanofluids of CuO, TiO₂, and Al₂O₃ nanoparticles. The results obtained for performance indexes were greater than 1 and the presence of ribs considerably increased the Nu and friction factor. Heat transfer behavior also depends on the rib shape, and therefore, rib shapes have been compared. The maximum Nu was found for the rectangular rib [75].

5.3. Investigations on Medicine Using Oil-Based Nanofluids

Ragvan et al. [106] conducted precautionary studies of a garlic oil nano-emulsion for preventing and treating dyslipidaemia, and reported reduced toxicity and improved efficacy using garlic oil. Gao et al. [107] and Hazer and Kalayci [108] reported that clove oil is a reducing agent that stabilizes the formation of silver nanoparticles. The outer layer of the nanoparticles coated with clove oil produces better antibacterial silver nanoparticles. The perpetual dielectric nature of a ZnO nanofluid at a high temperature can be used in industries as a coolant and lubricant [109]. The use of eco-friendly oils (minimum

quantity lubrication (MQL), nanoparticles with various harnesses, and vegetable oil) can be beneficial to solve environmental and human health issues raised by using conventional cutting fluids during machining processes [110–112].

5.4. Investigation on Solar Collectors Using Oil-Based Nanofluids

Adenutsi et al. [113] and Wang et al. [114,115] analyzed the performance of a gold/oil nanofluid used as the heat-transferring fluid in solar applications. The gold/oil nanofluid produced a 240% increase in photothermal conversion efficiency and was a better fluid in the absorption of indirect solar collectors.

Shen et al. [116] and Nimr and Dafaie [117] used mathematical modeling to verify that a nanofluid is an excellent solar radiation absorber. Khakrah et al. [118] investigated parabolic trough solar collectors (PTC) under the effect of various operational conditions for overall efficiency. They reported that, at the highest wind speed of 10 m/s, the thermal efficiency decreased by 7% compared to the still air, and 22% for heat transfer fluid (HTF) with a nanoparticle volume fraction of 5%. The relative exergy efficiency was increased by 19% through the addition of 5% nanoparticles. Gulzar et al. [119] observed that, instead of TiO_2 and Al_2O_3 -Therminol-55 nanofluids, the use of a hybrid nanofluid-enhanced photothermal conversion. A maximum temperature of 125.8 °C of Therminol-55 was recorded, whereas temperatures of 158.6 °C, 152.9 °C, and 149.6 °C were observed for 0.5 wt% hybrid (Al_2O_3 - TiO_2), 0.5 wt% Al_2O_3 -Therminol-55, and 0.1 wt% TiO_2 -Therminol-55 nanofluids, respectively. A hybrid nanofluid built on Therminol-55 was suited for high-temperature concentrating collectors, compared to the mono-nanofluid and base fluid. Wang et al. [120] studied the PTC system with an Al_2O_3 /synthetic oil nanofluid with variable heat flux distributions. The use of the Al_2O_3 /synthetic oil nanofluid had the potential to lower the solar absorber plate temperature and temperature gradient. The efficiency of the collectors of the PTC systems with Al_2O_3 /synthetic oil nanofluid was significantly higher as compared to synthetic oil. Loni et al. [121] reported a 12.93% increase in thermal efficiency using Al_2O_3 /thermal oil in a hemispherical cavity receiver as compared to a SiO_2 /thermal oil.

6. Oil-Based Review of Different Nanofluids Analyzed

6.1. Examination on Crude Oil-Based Nanofluids

Hendraningrat et al. [122] observed experimentally promising results and EOR by injecting a nanoparticle suspension. The testing was conducted in water-wet Berea core plugs for various nanofluid concentrations. Crude oil and nanofluid with concentrations of 0.01, 0.05, and 0.1 wt% were synthesized using synthetic brine. It was reported that the IFT is reduced as nanofluid concentration rises. Zhang et al. [123] investigated high salinity reservoir crude oil and brine solution nanofluid to replace crude oil with Berea sandstone. Berea sandstone enhances the efficiency by 50%, whereas the brine alone delivers a value of 17%. Alomair et al. [124] studied the effects of nanofluids to recover crude oil compared to the use of water flooding. The Al_2O_3 , SiO_2 , NiO, and TiO were added to saline water to form a nanofluid of different concentrations. The use of an Al_2O_3 nanofluid with a concentration of 0.05 wt% reduces the emulsion viscosity by 25%. The highest EOR was found for SiO_2 and Al_2O_3 nanofluids at 0.05 wt%. Table 7 represents the comparison of a previous investigation on crude-oil-based nanofluid.

Table 7. Comparison of previous investigations on crude-oil-based nanofluids.

Authors Name	Nanoparticle	Numerical/Experimental	Main Findings
Taborda et al. [54]	SiO ₂	Experimental	When the nanofluid is added, the highest viscosity reduction is obtained and a synergistic effect occurs which produces better viscosity reduction performance.
Radnia et al. [79]	Sulfonated graphene	Experimental	The value of IFT for aqueous phase with sulfonated graphene is lower than the IFT value of DI water.
Kuang et al. [80]	SiO _x , Al ₂ O ₃ , and TiO ₂	Experimental	SiO _x nanofluids were stable while the stability of Al ₂ O ₃ and TiO ₂ nanofluids depend on chemical agents. Pure Al ₂ O ₃ with 0.1 wt% nanofluid had a better performance than pure SiO _x nanofluid.
Dai [83]	SC – CO ₂	Experimental	The treatment and composition of SC – CO ₂ fracturing fluid decreased the permeability of cores to 85%.
Chen et al. [85]	Al ₂ O ₃	Experimental	Viscosity of crude is reduced to 10.4% at 0.2% of hydrophobic particle. Al ₂ O ₃ NPs reduces the IFT when ϕ is lower than 0.5%.
Alnarabiji et al. [86]	ZnO	Experimental	Mixing ZnO nanofluid with crude oil, the EOR is high. When the 0.01 wt% concentration of ZnO-NCs was used in the fluid, no permeability reduction took place.
Mohammadi et al. [99]	TiO ₂ , SiO ₂	Experimental	The doping of SiO ₂ reduces the particle size. An amount of 80% TiO ₂ nanofluid was optimal for the core flooding experiments.
Lee and Babadagli [125]	Al ₂ O ₃ , ZrO ₂	Experimental	Al ₂ O ₃ did not perform well in stabilizing emulsions. Al ₂ O ₃ +ZrO ₂ led to the rapid phase separation of emulsions.

6.2. Examination of Vegetable Oil-Based Nanofluids

Li et al. [126] reported that the trapping depth of vegetable-insulating nanofluids with an oil base is influenced by the nanoparticle surfactant polarization. Su et al. [70], Padmini et al. [127], and Li et al. [128] evaluated cutting force and temperature using the nanofluid MQL with vegetable oil and ester oil as base fluids. At high cutting speed, the performance of graphite-LB2000 revealed a reduction in the cutting force and temperature, and was superior to the graphite-Pri Eco 6000 nanofluid. The turning of AISI 1040 steel using cutting fluids as vegetable-oil-based nano was examined by Rapeti et al. [129]. Improved machining was seen at a feed rate of 0.14 mm/rev and a cutting speed of 40 m/min using 0.5% coconut oil nano-molybdenum sulfide with 0.5% nanoparticle concentration.

Desari and Davoodi [57] investigated vegetable oils as a lubricant for its biodegradability and non-toxicity in the metal-forming process for reduction in friction losses and extreme pressure capabilities. A diverse concentration of nanofluids was formed by dispersing the CuO and SiO₂ nanoparticles of rapeseed and soybean oils with two metal-forming

lubricants, and their lubrication performance was compared. Mechiri et al. [76] analyzed the vegetable oils and reported that the Brownian motion of the particles enhanced thermal conductivity. High viscosity leads to the lubrication property and reduces the energy input, as well as the generation of heat during grinding. Table 8 represents the comparison of the previous investigations on vegetable-oil-based nanofluids.

Table 8. Comparison of previous investigations on vegetable-oil-based nanofluids.

Authors Name	Nanoparticles	Numerical/ Experiment	Main Findings
Su et al. [70]	Graphite	Experiment	Increase in mass fraction of nano-graphite resulted in the reduction in cutting force and temperature, irrespective of the type of base oil.
Mechiri et al. [76]	Cu – Zn	Experiment	Hybrid Cu – Zn (50:50) has the advantage of having less density and high thermal conductivity as compared to Cu – Zn (25:75) and Cu-Zn (75:25).
Gao [110]	CNT	Experiment	Among the six surfactants, the CNT nanofluids with APE-10 have the highest viscosity, lowest friction coefficient and minimum roughness value. The addition of surfactant can increase the viscosity of the CNT nanofluids.
Yuan et al. [112]	Diamond, Cu and SiC	Experiment	Nano-Diamond and nano-Cu have better results in reducing cutting forces than nano-SiC.
Li et al. [126]	Fe ₃ O ₄	Experiment	Covalent bonding between oleic acid and Fe ₃ O ₄ crystals prevents agglomeration of Fe ₃ O ₄ nanoparticles and also improves the compatibility between the nanoparticles and the vegetable insulating oil.
Padmini et al. [127]	CC+nMoS ₂	Experiment	Maximum enhancement in thermal conductivity, specific heat and heat transfer coefficient in case of CC+nMoS ₂ is 2.5%, 0.98% and 3.54% from base fluids, respectively.
Li et al. [128]	Fe ₃ O ₄	Experiment	The appropriate nanofluid MQL parameter could enhance the lubrication and cooling properties of the oil film to improve the surface quality and reduce the surface roughness.
Lv et al. [130]	Fe ₃ O ₄	Experiment	The AC breakdown strength of Fe ₃ O ₄ nanoparticles and NF-8 is the highest one and up to 1.4 times of that the base oil.

6.3. Study on Pure Oil-Based Nanofluids

Arani et al. [68] experimentally investigated the HTC for various parameters (Re, nanofluid particle concentration, and tube diameter ratio). They revealed that the HTC and

pressure increased by replacing pure oil with nanofluid. Razi et al. [61] and Jiang et al. [131] analyzed CuO-base oil nanofluids with particle weight fractions between 0.2 and 2%. They reported that the inclusion of nanoparticles in the base fluid increased the thermal conductivity of the nanofluid as the specific heat capacity decreased. An increase in HTC by 12.7% was observed for a specific nanoparticle concentration compared to pure oil. Table 9 represents the comparison of a previous investigation on pure oil-based nanofluids.

Table 9. Comparison of previous investigations on pure oil-based nanofluids.

Authors Name	Nanoparticles	Numerical/ Experiment	Main Findings
Jafarimoghaddam et al. [43]	Ag	Experiment	The HTC of nanoparticles suspended in the base oil is higher than the base oil.
Moraveji and Hejazian [62]	CuO	Numerical	A combination of the two enhancing methods made a significant improvement on heat transfer.
Beheshti et al. [67]	MWCNT	Experiment	The viscosity of nanofluids is lower than that of pure oil. The thermal conductivity of pure oil decreased, and that of nanofluids increased.
Jafarimoghaddam et al. [68]	Ag	Experiment	Silver-oil nanofluids exhibit a higher viscosity than pure oil. HTC increases with increasing Reynolds number due to increasing the fluid velocity.
Aberoumand et al. [73]	Ag	Experiment	The average Nusselt number was about 13.4% higher than the simple annular tube. The specific HTC decreases in the presence of low concentrations of the Ag/oil nanofluid.
Jafarimoghaddam et al. [132]	Al	Experiment	The average increase of Nusselt number for Al/oil nanofluid was found to be about 16.4%.
Jia et al. [3]	MoFe ₂ O ₄ -NiFe ₂ O ₄	Experiment	The friction coefficient of MoFe ₂ O ₄ and NiFe ₂ O ₄ nano-oil was lower than that of pure oil. MoFe ₂ O ₄ nano-oil makes the biggest impact on refrigeration performance.

6.4. Exploration on Palm-Oil-Based Nanofluids

Li et al. [107] selected palm oil as the base oil of MQL cooling. Various nanofluids with volume fractions ranging from 0.5 to 4% were made by the nanoparticles of carbon nanotube (CNT) for MQL cooling grinding of a Ni-based alloy to determine the optimum heat transfer and lubrication performance. Li et al. [133] investigated palm oil as the MQL base oil. The MoS₂, ZrO₂, CNT, PCD, Al₂O₃, and SiO₂ nanoparticles were added to form nanofluids. The minimum grinding force ratio of 0.365 was achieved for SiO₂, followed by MoS₂ nanofluid with a ratio of 0.367, while the PCD nanofluid showed the best ratio of grinding force of 0.40. Li et al. [126,134] studied palm oil and found an increase in thermal conductivity because of Brownian motion of nanoparticles and revealed that the higher viscosity of the nanofluid promotes the lubrication effect that leads to the lower energy input and less grinding heat. Table 10 represents the comparison of a previous investigation on palm-oil-based nanofluids.

Table 10. Comparison of previous investigations on palm-oil-based nanofluids.

Authors Name	Nanoparticle	Numerical/ Experimental	Main Findings
Javed et al. [33]	CuO	Experimental	The maximum enhancement was observed for 0.7% nanoparticles concentration.
Wang et al. [74]	MoS ₂ , ZrO ₂ , CNT, PCD, Al ₂ O ₃ , SiO ₂	Experimental	CNT nanoparticles have the highest thermal conductivity. Adding nanoparticles to the base fluid can increase the viscosity of the base fluid. The density of MoS ₂ nanoparticles is higher than that of PCD nanoparticles.
Fontes et al. [96]	CNT	Experimental	The 4 vol.% nanofluid possesses the highest viscosity. The addition of nanoparticles into the base fluid can significantly increase the HTC.
Hussein et al. [100]	TiO ₂	Experimental	The viscosity of the nanofluids increases as nanofluid volume concentration increases. Heat transfer enhancement was observed when nanoparticles were added to the pure oil.

6.5. Exploration on Engine-Oil-Based Nanofluids

Wang et al. [74] employed various nanoparticles in traditional engine oil for developing a novel nanofluid cooling medium, and analyzed the heat transfer rate of engine oil and nanofluids. Mohammad and Kandasamy [135] showed that engine-oil-based nanofluids have a significant impact on temperature distribution by augmenting the nanoparticle volume fraction. Derakhshan and Behabadi [45] and Rehman et al. [136] employed a 3D flow of rotating water and engine-oil-based nanofluid for the analysis by varying the nanometer-sized single-walled carbon nanotubes (SWCNT) and MWCNT. The SWCNT delivers a higher skin friction and Nu because of their higher density and thermal conductivity.

Asadi et al. [77], Tao et al. [137], and Asadi et al. [138] examined the rate of heat transfer of an engine-oil-based nanofluid lubricating oil, with concentrations varying from 0.25 to 2%. They reported that the dynamic viscosity of the nano-lubricant increases as the solid concentration is increased. Finally, they concluded that nanofluids are advantageous for heat transfer applications used as a coolant fluid. Pryazhnikov et al. [139] analyzed the thermal conductivity coefficient of Al₂O₃, TiO₂, SiO₂, ZrO₂, CuO, and diamond particles based on water, ethylene glycol, and engine oil.

They also found that the base liquid influences the thermal conductivity of the nanofluids. Ghazvini et al. [64] investigated the effects of utilizing nano-diamond particles with engine oil as the base fluid, and revealed higher heat transfer rates and pressure drops by adding nanoparticles. Isfahani et al. [72] and Mashhadi et al. [140] examined the behavior of engine oil using various types of hybrid nano-additives, and reported that the viscosity of the nanofluid goes up by increasing the nano-additives concentration.

Wang et al. [120], Dinesh et al. [141], He et al. [142], and Quercia et al. [143] stated that the use of a nanofluid made with engine oil as the base fluid boosted the lubrication properties. Sgroi et al. [144] reported that fuel consumption was reduced by 0.9% compared to traditional engine oil. Pourfattah and Asadi [145] analyzed the ZnO and MgO-engine oil nanofluid for thermophysical and heat transfer characteristics as coolants and lubricants in various engineering applications. They observed that the nanofluid with ZnO raises the dy-

namic viscosity, and in laminar flow regimes the heat transfer performance is good. Table 11 represents the comparison of a previous investigations on engine-oil-based nanofluids.

Table 11. Comparison of previous investigations on engine-oil-based nanofluids.

Authors Name	Nanoparticle	Numerical/ Experimental	Main Findings
Vasheghani et al. [35]	Alumina	Experimental	Addition of 3 wt% of γ -Al ₂ O ₃ was found to improve thermal conductivity by 37.49%. γ -Al ₂ O ₃ -based engine oil has better performance as compared to α -Al ₂ O ₃ -based engine oil.
Aghaei et al. [54]	CuO-MWCNTs	Experimental	The nanofluid viscosity decreases with temperature increment.
Isfahani et al. [72]	Al ₂ O ₃ -MWCNTs	Experimental	The maximum deviations of relative viscosity occur between temperatures of 25 °C and 50 °C. The relative viscosity of Al ₂ O ₃ -MWCNTs/SAE40 is significantly more.
Wang et al. [74]	Copper and diamond	Numerical	The combination Cu-oil has a better performance as compared to traditional oil. Diamond-oil-based nanofluid has a better performance as compared to Cu-oil.
Asadi et al. [77]	Mg(OH) ₂ – MWCNT	Experimental	The thermal conductivity of the nanofluid enhances as the solid concentration increases. Using this nanofluid would be advantageous in cooling applications.
Mohammad and Kandasamy [135]	Cu, Al ₂ O ₃ and SWCNTs	Numerical	The temperature of the nanofluids with different nanoparticle shapes increases. Ethylene glycol and engine oil have a unique impact on temperature distribution.
Rehman et al. [136]	SWCNT, MWCNTs	Numerical	MWCNTs proved to be more effective in rapid heat transfer at the surface. SWCNTs have high density compared to MWCNTs.
Asadi and Aberoumand [138]	MgO-MWCNT	Experimental	A maximum increase of 65% in HTC was found at a temperature of 40 °C.

6.6. Investigations on Mineral-Oil-Based Nanofluids

Sundar et al. [39] and Gara and Zou [146] experimentally investigated the tribological properties of ZnO nanofluids in paraffinic mineral oil and reported a reduction in friction, which enhanced the dispersibility and stability of the nanofluids. Ingole et al. [40] studied applications of the mineral-based nano-oils on two domestic refrigerator compressors. The performance of the two compressors was enhanced by 5.6 and 5.3%, respectively, compared to mineral oil. Fontes et al. [147] and Hameed et al. [148] investigated MWCNT-based nanofluids to determine the Nu for the same Grashof number (Gr), and reported that the nanofluids presented better convection characteristics. The maximum increase in the convection HTC was 23% for diamond nanofluids with a higher volumetric concentration. Lv et al. [149] concluded that thermal conductivity increased with nanoparticles. Table 12 represents the comparison of previous investigations on mineral-oil-based nanofluids.

Table 12. Comparison of previous investigations on mineral-oil-based nanofluids.

Authors Name	Nanoparticle	Numerical/ Experimental	Main Findings
Ingole et al. [66]	TiO ₂	Experimental	Base oil with 2 wt% showed the highest HTC.
Beheshti et al. [67]	MWCNT	Experimental	Increasing the concentration led to an increase in the density of nanofluids. The highest thermal conductivity obtained for 0.01 mass% was at 20 °C.
Fontes al. [96]	MWCNT, Diamond	Experimental	The dynamic viscosity increases with increasing the nanoparticle concentration.
Fontes et al. [147]	MWCNT, Diamond	Numerical	The mean Nusselt number increased with the Prandtl number of the nanofluids.
Lv et al. [149]	TiO ₂	Experimental	The enhancement on the thermal conductivity is due to the formation of clusters.

6.7. Examination on Thermal-Oil-Based Nanofluids

Asadi et al. [150] determined the rate of heat transfer for an Al₂O₃-MWCNT/thermal oil hybrid nanofluid to have concentrations in the range of 0.125 to 1.5%, and temperatures from 25 °C to 50 °C. They reported that the application of nanofluid is prolific in laminar and turbulent flow as compared to base fluid. Loni et al. [151–153] examined the nanofluids Cu/thermal oil, Al₂O₃/thermal oil, SiO₂/thermal oil, and TiO₂/thermal oil. They saw that thermal efficiency was reduced when nanoparticle volume concentrations were increased, and the exergetic efficiency was enhanced by increasing nanofluid concentrations. The Cu/thermal oil nanofluid also delivered the highest exergy in the investigated nanofluid in a cylindrical cavity receiver.

Herper and Entel [154] studied four types of nanofluids for the thermal properties of Al₂O₃, Fe₃O₄, SiO₂, and SiC nanoparticles in thermal oils. An augmentation in the thermal conductivity of oil by 8% was reported when 0.5 wt.% of aluminum nitride nanoparticles were dispersed, and cooling was enhanced by 20%. In the thermal-oil-based nanofluids with 0.08% < φ < 0.39%, the dielectric breakdown voltage was three times higher than that of pure thermal oil [103]. Beheshti et al. [67] experimentally determined the effect of oxidized MWCNT on the properties of thermal oil, and a decreased breakdown in voltage was reported as the concentration increased. Aberoumand et al. [73] examined the rate of heat transfer of an oil-based silver nanofluid with parameter temperatures ranging from 40 °C to 100 °C and mass fractions of 0.12 to 0.72%. The enhancement in viscosity depends on temperature, whereas the specific heat capacity decreases as the mass concentration of nanofluids increases. Sadegh et al. [73] and Mohammadi et al. [155] and found that the thermal conductivity of a thermal-oil-based nanofluid was enhanced with temperature, whereas the specific heat capacity reduced as the mass concentration increased. Qin et al. [58] synthesized stearic acid-modified CuS (SA-CuS) nanoparticles with a uniform diameter of 60 nm by a facile two-phase approach Table 13 represents the comparison of a previous investigation on thermal-oil-based nanofluids.

Table 13. Comparison of previous investigations on thermal-oil-based nanofluids.

Authors Name	Nanoparticle	Numerical/ Experimental	Main Findings
Hekmatipour et al. [32]	CuO	Experimental	The nanoparticles were more in favor of heat transfer enhancement rather than pressure drop. The maximum performance index was approximately 61% at $\varphi = 1.5\%$.
Sokhansefat et al. [45]	Al ₂ O ₃ , SiO ₂	Experiment	The average thermal efficiency of the cylindrical cavity receiver using the Al ₂ O ₃ /thermal oil nanofluid was highest.
Qin et al. [58]	CuS	Experimental	The thermal conductivity enhancement was 20.5% for $\varphi = 0.04\%$ at $T = 30\text{ }^{\circ}\text{C}$.
Derakhshan and Behabadi [71]	MWCNT	Experimental	The maximum effect of nanoparticles on enhancement of heat transfer was found using a horizontal plain tube.
Gholami et al. [75]	MWCNT	Numerical	Sharp angles of rib caused heat transfer enhancement. The rectangular and parabolic ribs had the maximum and minimum amounts of average Nu.
Gulzar et al. [119]	Al ₂ O ₃ , TiO ₂	Experiment	Nanoparticles had significantly less absorbance in the UV region. TiO ₂ nanofluids exhibited better optical properties than Al ₂ O ₃ .
Loni et al. [156]	MWCNT	Experiment	The thermal efficiency of the hemispherical cavity receiver using the MWCNT/oil nanofluid was higher than base oil.
Asadi et al. [138]	MgO-MWCNT	Experiment	The maximum increase in dynamic viscosity was 65% at $T = 40\text{ }^{\circ}\text{C}$. The nanoparticles could be attributed to the higher conductivity of MWCNT and MgO nanoparticles.

7. Comparative Study

A comparison of various nanoparticles was conducted based on Nu generated where the base fluid used was pure oil. Figure 2 shows the variation of Nu for different Re using various nanofluids. It was revealed that SiO₂/oil nanofluid delivered the maximum Nu, followed by Al₂O₃/oil, ZnO/oil, CuO/oil, and pure oil, respectively.

The variation of Nu for different Re is presented in Figure 3, which reveals that the value of the Nu is higher for base fluids of oil + water, compared to plain water. The probable reason for the higher Nu is that oil + water has a high dynamic viscosity compared to water, which results in an augmentation in heat transfer capabilities. The comparative studies in the literature review also show that hybrid nanofluids deliver augmented heat transfer as compared to simple nanofluids, which are boosted by a rise in Re; as represented in Figure 4.

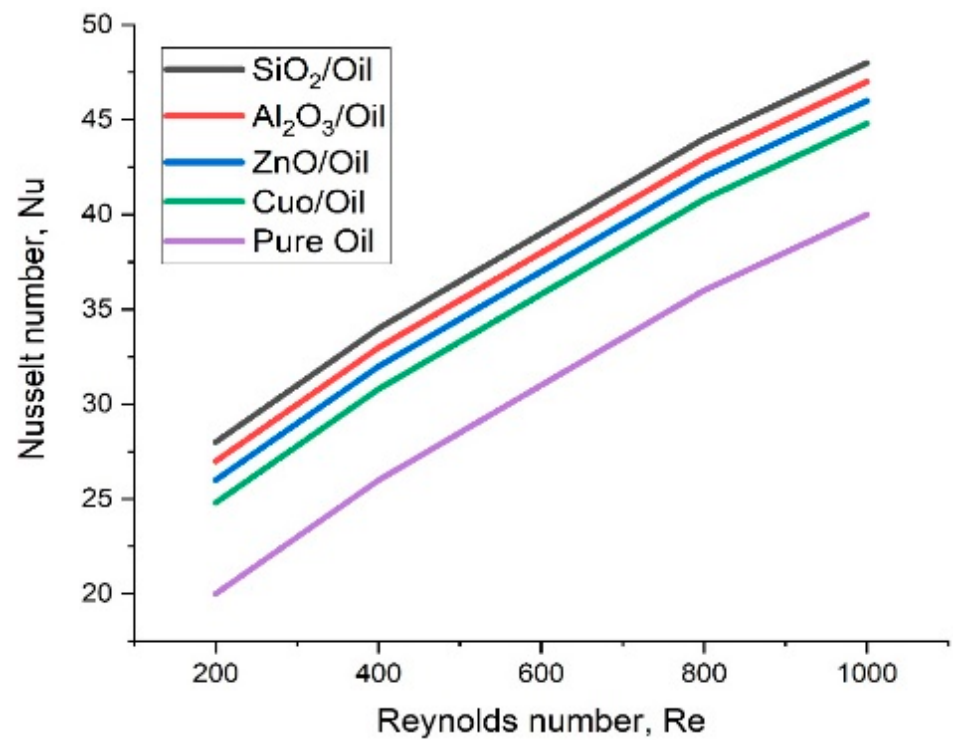


Figure 2. Comparison of Nu vs. Re with different oil-based nanofluids.

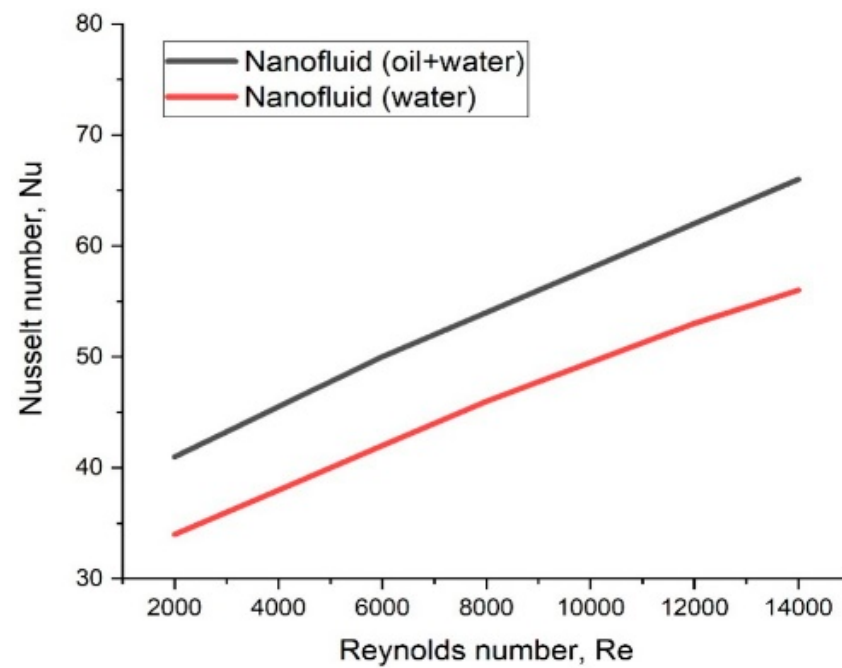


Figure 3. Comparison of Nu vs. Re with water and oil + water-based nanofluids.

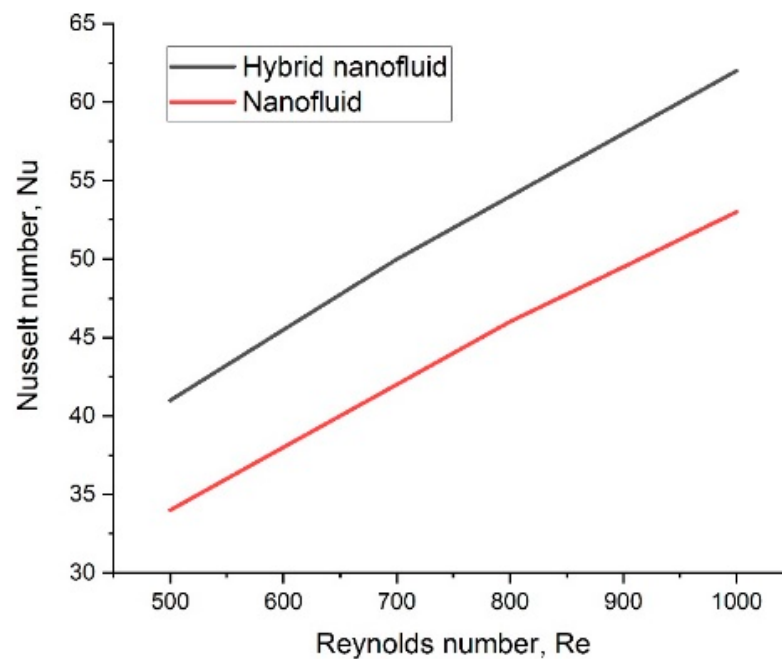


Figure 4. Comparison of Nu vs. Re with simple and hybrid nanofluids.

It is evident from the comparative study, as shown in Figure 3, that the oil-based nanofluids deliver added thermal conductivity as compared to the base fluid. The nano particles concentrations is also a major parameters that can affect the thermal conductivity of nanofluids, as shown in Figure 5. The literature review also revealed that the thermal conductivity of hybrid Ag – WO_3 /mineral-oil-based nanofluids is higher than the amine-treated graphene mineral-oil-based and simple MWCNT/mineral-oil-based fluid, as shown in Figure 6. Figure 7 shows that the thermal conductivity of Al_2O_3 – MWCNT/thermal-oil-based nanofluids is higher than MgO – MWCNT/thermal oil and simple MWCNT/thermal oil-based nanofluids. For all nanofluids, the thermal conductivity also increases with temperature because the Brownian motion of the particles is greater at elevated temperatures.

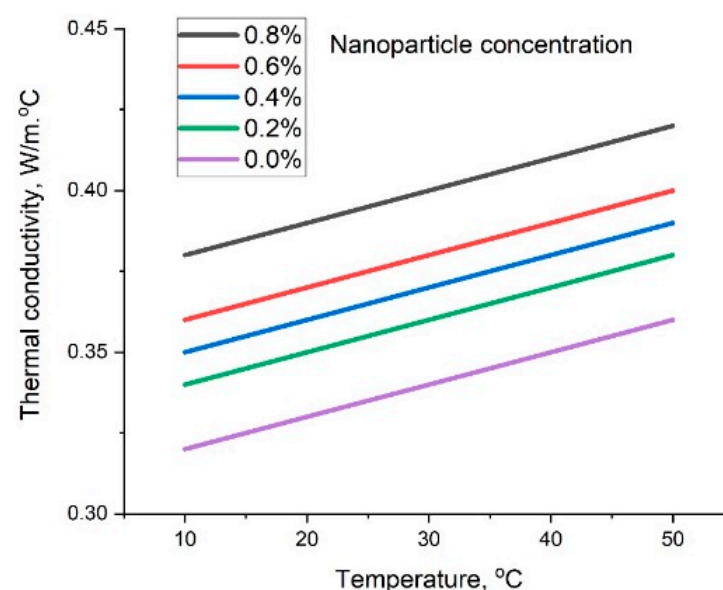


Figure 5. Comparison of thermal conductivity vs. temperature with nanoparticle concentration.

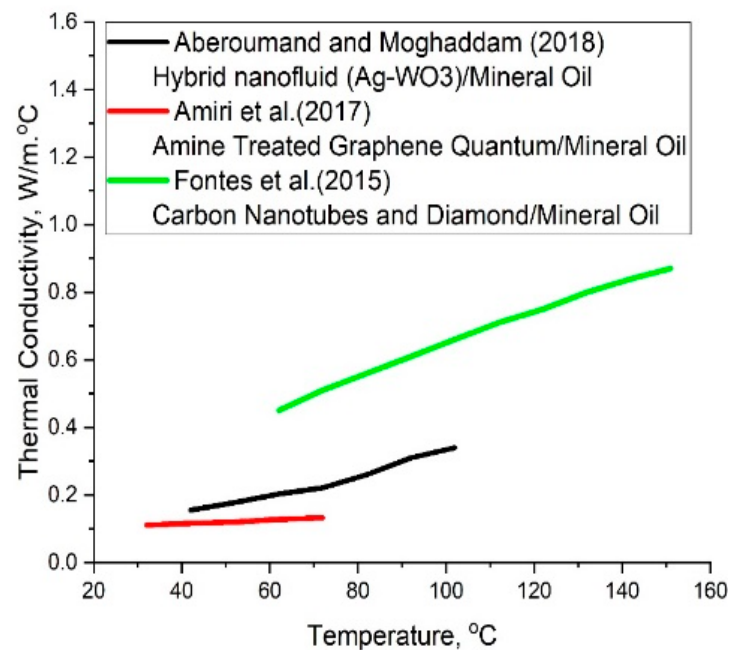


Figure 6. Comparison of thermal conductivity vs. temperature with various nanoparticle/mineral oil.

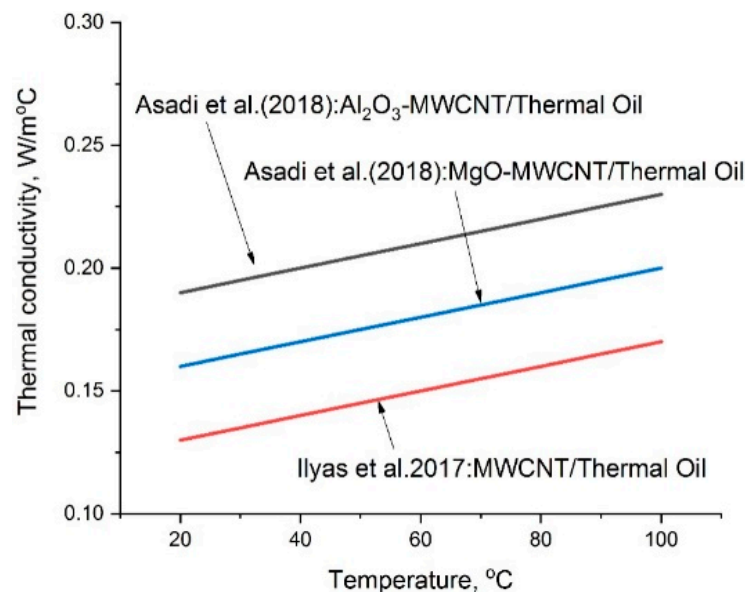


Figure 7. Comparison of thermal conductivity vs. temperature with various nanoparticle/thermal oil.

8. Research Gaps, Challenges, and Future Works

This review of oil-based nanofluids determined the benefits of switching the nanofluid base from water to oil. These prolific outcomes were analyzed in the fields of solar thermal systems, heat exchangers, lubrication in grinding, refrigeration, and engines. The results revealed the effective performance of oil-based nanofluids for different oils, nanoparticles, and concentrations used in specific processes. The review also identified gaps in the analyzed literature. Future work in these domains should focus on sustainability analysis concerning the use of oil as the base fluid in terms of cost analysis, emissions from oil when heated, and energy consumption in driving the high viscosity oil through the channel.

9. Conclusions

This study reviewed the literature addressing the use of nanofluid/oil and the major conclusions drawn from the survey are summarized as follows:

- The use of nanoparticles suspended in oil leads to a remarkable reduction in the specific energy requirement during grinding operation.
- Nanoparticles with Cu and Zn as the chief constituents have high and low densities, respectively, whereas hybrid nanoparticles with the same concentrations have average densities. Compared to nano-SiC, nano-diamond and nano-copper have better results in reducing the cutting forces.
- The HTC of nanofluids is improved by volume concentration and temperature augmentation. The maximum convective heat transfer enhancement for SiO₂ is 81%, compared to the base fluid at a volume concentration and temperature of 3.0 and 70 °C, respectively.
- The use of nanoparticles enhances thermal conductivity, anti-frictional properties, and cooling-lubrication characteristics of various oils. Similarly, the wettability of the oil is significantly enhanced with nano-suspension.
- The thermal conductivity of water-based nanofluids is improved by 19.14% and the ethylene glycol-based nanofluid is improved by 11.85%. Likewise, the viscosity of water-based and ethylene-glycol-based nanofluids is enhanced by 1.70 and 1.42 times, respectively.
- Silver/oil nanofluids are prolific in increasing the Nu in a thermal system. The thermal conductivity of nanofluids is directly proportional to the nanoparticle concentration. The stability of Al₂O₃ and TiO₂ nanofluids depends on the concentration of the chemical agents added. The stability of the nanofluids increases up to $\varphi = 0.1\%$; with a further increase in φ , the stability starts to decrease.
- Adding nanoparticles with different volume fractions to the pure oil notably enhances the heat transfer and friction factor.
- A higher thermal efficiency is seen using the Al₂O₃/thermal oil nanofluid compared to the SiO₂/thermal oil nanofluid in a cylindrical cavity receiver. It is recommended that the cylindrical cavity receiver should be used with the Al₂O₃/thermal oil nanofluid to obtain a higher thermal efficiency.
- More experimental data is still needed to fill in the gaps in the knowledge.

Author Contributions: Conceptualization, S.K., M.S. (Mridul Sharmaand), A.B., S.S. and A.K.; methodology, R.M., T.A. and S.S.; software, T.A., A.K., S.S. and N.K.G.; validation, S.K., M.S. (Mridul Sharmaand), A.B., S.S., T.A. and A.K.; formal analysis, M.S. (Mridul Sharmaand), T.A., A.K. and M.S. (Mohsen Sharifpur); investigation, R.M., S.S. and N.K.G.; resources, M.S. (Mohsen Sharifpur); data curation, S.K., M.S. (Mridul Sharmaand), A.B. and A.K.; writing—original draft preparation, S.K., M.S. (Mridul Sharmaand), S.S., A.B. and A.K.; writing—review and editing, A.K., R.M., S.S. and T.A.; visualization, N.K.G.; supervision, M.S. (Mohsen Sharifpur); project administration, A.K. and R.M.; funding acquisition, A.K. and R.M. All authors have read and agreed to the published version of the manuscript.

Funding: This research received no external funding.

Data Availability Statement: Not applicable.

Conflicts of Interest: The authors declare no conflict of interest.

Nomenclature

	Diameter of nanoparticles
Gr	<i>Grashof number</i>
	Nusselt number
	Reynolds number
	Concentration of solid particles

Abbreviations

CNT	Carbon nanotubes
EOR	Enhanced oil recovery
IFT	Interfacial tension
HTF	Heat transfer fluid
HTC	Heat transfer coefficient
MQL	Minimum quantity lubrication
MWCNT	Multi-walled carbon nanotubes
PTC	Parabolic trough solar collector
SWCNT	Single-walled carbon nanotubes

References

- Ahmed, H.E.; Ahmed, M.I.; Yusoff, M.Z.; Hawlader, M.N.A.; Al-Ani, H. Experimental study of heat transfer augmentation in non-circular duct using combined nanofluids and vortex generator. *Int. J. Heat Mass Transf.* **2015**, *90*, 1197–1206. [\[CrossRef\]](#)
- ManojKumar, K.; Ghosh, A. Synthesis of MWCNT nanofluid and evaluation of its potential besides soluble oil as micro cooling-lubrication medium in SQL grinding. *Int. J. Adv. Manuf. Technol.* **2015**, *77*, 1955–1964. [\[CrossRef\]](#)
- Jia, T.; Wang, R.; Xu, R. Performance of MoFe₂O₄-NiFe₂O₄/Fullerene-added nano-oil applied in the domestic refrigerator compressors. *Int. J. Refrig.* **2014**, *45*, 120–127. [\[CrossRef\]](#)
- Kumar, S.; Gautam, S.K.; Kumar, A.; Maithan, R.; Kumar, A. Sustainability assessment of different nanoparticle for heat exchanger applications: An intuitionistic fuzzy combinative distance-based assessment method. *Acta Innov.* **2021**, *40*, 44–63. [\[CrossRef\]](#)
- Sheremet, M.A.; Revnin, C.; Pop, I. Natural convective heat transfer through two entrapped triangular cavities filled with a nanofluid: Buongiorno's mathematical model. *Int. J. Mech. Sci.* **2017**, *133*, 484–494. [\[CrossRef\]](#)
- Léal, L.; Miscevic, M.; Lavieille, P.; Amokrane, M.; Pigache, F.; Topin, F.; Nogarède, B. International Journal of Heat and Mass Transfer An overview of heat transfer enhancement methods and new perspectives: Focus on active methods using electroactive materials. *Int. J. Heat Mass Transf.* **2013**, *61*, 505–524. [\[CrossRef\]](#)
- Sofiah, A.G.N.; Samykano, M.; Pandey, A.K.; Kadirgama, K.; Sharma, K.; Saidur, R. Immense impact from small particles: Review on stability and thermophysical properties of nanofluids. *Sustain. Energy Technol. Assess.* **2021**, *48*, 101635. [\[CrossRef\]](#)
- Kumar, N.; Bharti, A.; Saxena, K.K. A re-investigation: Effect of powder metallurgy parameters on the physical and mechanical properties of aluminium matrix composites. *Mater. Today Proc.* **2021**, *44*, 2188–2193. [\[CrossRef\]](#)
- Kumar, S.; Shandilya, M.; Chauhan, A.; Maithani, R.; Kumar, A. Experimental analysis of zinc oxide/water/ethylene glycol-based nanofluid in a square duct roughened with inclined ribs. *J. Enhanc. Heat Transf.* **2020**, *27*, 687–709. [\[CrossRef\]](#)
- Ranga Babu, J.A.; Kumar, K.K.; Srinivasa Rao, S. State-of-art review on hybrid nanofluids. *Renew. Sustain. Energy Rev.* **2017**, *77*, 551–565. [\[CrossRef\]](#)
- Kumar, N.; Gupta, S.K.; Sharma, V.K. Application of phase change material for thermal energy storage: An overview of recent advances. *Mater. Today Proc.* **2021**, *44*, 368–375. [\[CrossRef\]](#)
- Ahmed, H.E.; Mohammed, H.A.; Yusoff, M.Z. An overview on heat transfer augmentation using vortex generators and nanofluids: Approaches and applications. *Renew. Sustain. Energy Rev.* **2012**, *16*, 5951–5993. [\[CrossRef\]](#)
- Kumar, S.; Kumar, A. A comprehensive review on the heat transfer and nanofluid flow characteristics in different shaped channels. *Int. J. Ambient Energy* **2021**, *42*, 345–361. [\[CrossRef\]](#)
- Navaei, A.S.; Mohammed, H.A.; Munisamy, K.M.; Yarmand, H.; Gharehkhani, S. Heat transfer enhancement of turbulent nanofluid flow over various types of internally corrugated channels. *Powder Technol.* **2015**, *286*, 332–341. [\[CrossRef\]](#)
- Haridas, D.; Rajput, N.S.; Srivastava, A. Interferometric study of heat transfer characteristics of Al₂O₃ and SiO₂-based dilute nanofluids under simultaneously developing flow regime in compact channels. *Int. J. Heat Mass Transf.* **2015**, *88*, 713–727. [\[CrossRef\]](#)
- Dogonchi, A.S.; Ganji, D.D. Effect of Cattaneo–Christov heat flux on buoyancy MHD nanofluid flow and heat transfer over a stretching sheet in the presence of Joule heating and thermal radiation impacts. *Indian J. Phys.* **2018**, *92*, 757–766. [\[CrossRef\]](#)
- Yang, Y.-T.; Tang, H.-W.; Zeng, B.-Y.; Jian, M.-H. Numerical simulation and optimization of turbulent nanofluids in a three-dimensional arc rib-grooved channel. *Numer. Heat Transf. Part A Appl.* **2016**, *70*, 831–846. [\[CrossRef\]](#)
- Vanaki, S.M.; Mohammed, H.A. Numerical study of nanofluid forced convection flow in channels using different shaped transverse ribs. *Int. Commun. Heat Mass Transf.* **2015**, *67*, 176–188. [\[CrossRef\]](#)
- Parashar, A.K.; Gupta, A. Investigation of the effect of bagasse ash, hooked steel fibers and glass fibers on the mechanical properties of concrete. *Mater. Today Proc.* **2021**, *44*, 801–807. [\[CrossRef\]](#)
- Minkowycz, W.J.; Sparrow, E.M.; Abraham, J.P. *Nanoparticle Heat Transfer and Fluid Flow*; Advances in Numerical Heat Transfer: Computational and Physical Processes in Mechanics and Thermal Sciences; Taylor & Francis: Abingdon, UK, 2012; ISBN 9781439861929.
- Ahmed, H.E.; Ahmed, M.I.; Yusoff, M.Z. Heat transfer enhancement in a triangular duct using compound nanofluids and turbulators. *Appl. Therm. Eng.* **2015**, *91*, 191–201. [\[CrossRef\]](#)
- Ho, C.J.; Liu, W.K.; Chang, Y.S.; Lin, C.C. Natural convection heat transfer of alumina-water nanofluid in vertical square enclosures: An experimental study. *Int. J. Therm. Sci.* **2010**, *49*, 1345–1353. [\[CrossRef\]](#)

23. Petukhov, B.S. Heat Transfer and Friction in Turbulent Pipe Flow with Variable Physical Properties. In *Advances in Heat Transfer*; Hartnett, J.P., Irvine, T.F., Eds.; Elsevier: Amsterdam, The Netherlands, 1970; Volume 6, pp. 503–564.
24. Gnielinski, V. New equations for heat and mass transfer in the turbulent flow in pipes and channels. *NASA STI/Recon Tech. Rep. A* **1975**, *41*, 8–16.
25. Dittus, F.W.; Boelter, L.M.K. Heat transfer in automobile radiators of the tubular type. *Int. Commun. Heat Mass Transf.* **1985**, *12*, 3–22. [[CrossRef](#)]
26. El Bécaye Maïga, S.; Tam Nguyen, C.; Galanis, N.; Roy, G.; Maré, T.; Coqueux, M. Heat transfer enhancement in turbulent tube flow using AlO nanoparticle suspension. *Int. J. Numer. Methods Heat Fluid Flow* **2006**, *16*, 275–292. [[CrossRef](#)]
27. Duangthongsuk, W.; Wongwises, S. Heat transfer enhancement and pressure drop characteristics of TiO₂–water nanofluid in a double-tube counter flow heat exchanger. *Int. J. Heat Mass Transf.* **2009**, *52*, 2059–2067. [[CrossRef](#)]
28. Suresh, S.; Venkataraj, K.P.; Selvakumar, P.; Chandrasekar, M. Effect of Al₂O₃–Cu/water hybrid nanofluid in heat transfer. *Exp. Therm. Fluid Sci.* **2012**, *38*, 54–60. [[CrossRef](#)]
29. Sundar, L.S.; Singh, M.K.; Sousa, A.C.M. Enhanced heat transfer and friction factor of MWCNT–Fe₃O₄/water hybrid nanofluids. *Int. Commun. Heat Mass Transf.* **2014**, *52*, 73–83. [[CrossRef](#)]
30. Madhesh, D.; Parameshwaran, R.; Kalaiselvam, S. Experimental investigation on convective heat transfer and rheological characteristics of Cu–TiO₂ hybrid nanofluids. *Exp. Therm. Fluid Sci.* **2014**, *52*, 104–115. [[CrossRef](#)]
31. Hwang, Y.; Park, H.S.; Lee, J.K.; Jung, W.H. Thermal conductivity and lubrication characteristics of nanofluids. *Curr. Appl. Phys.* **2006**, *6*, e67–e71. [[CrossRef](#)]
32. Hekmatipour, F.; Jalali, M.; Hekmatipour, F.; Akhavan-Behabadi, M.A.; Sajadi, B. On the convection heat transfer and pressure drop of copper oxide-heat transfer oil Nanofluid in inclined microfin pipe. *Heat Mass Transf.* **2019**, *55*, 433–444. [[CrossRef](#)]
33. Javed, M.; Shaik, A.H.; Khan, T.A.; Imran, M.; Aziz, A.; Ansari, A.R.; Chandan, M.R. Synthesis of stable waste palm oil based CuO nanofluid for heat transfer applications. *Heat Mass Transf.* **2018**, *54*, 3739–3745. [[CrossRef](#)]
34. Hwang, Y.; Lee, J.K.; Lee, C.H.; Jung, Y.M.; Cheong, S.I.; Lee, C.G.; Ku, B.C.; Jang, S.P. Stability and thermal conductivity characteristics of nanofluids. *Thermochim. Acta* **2007**, *455*, 70–74. [[CrossRef](#)]
35. Vasheghani, M.; Marzbanrad, E.; Zamani, C.; Aminy, M.; Raissi, B.; Ebadzadeh, T.; Barzegar-Bafrooei, H. Effect of Al₂O₃ phases on the enhancement of thermal conductivity and viscosity of nanofluids in engine oil. *Heat Mass Transf. Stoffuebertragung* **2011**, *47*, 1401–1405. [[CrossRef](#)]
36. Yu, W.; Xie, H.; Li, Y.; Chen, L.; Wang, Q. Experimental investigation on the thermal transport properties of ethylene glycol based nanofluids containing low volume concentration diamond nanoparticles. *Colloids Surfaces A Physicochem. Eng. Asp.* **2011**, *380*, 1–5. [[CrossRef](#)]
37. Gholamipour-Shirazi, A.; Carvalho, M.S.; Fossum, J.O. Controlled microfluidic emulsification of oil in a clay nanofluid: Role of salt for Pickering stabilization. *Eur. Phys. J. Spec. Top.* **2016**, *225*, 757–765. [[CrossRef](#)]
38. Farbod, M.; Mohammadian, A.; Ranjbar, K.; Kouhpeymani Asl, R. Effect of Sintering on the Properties of γ -Brass (Cu₅Zn₈) Nanoparticles Produced by the Electric Arc Discharge Method and the Thermal Conductivity of γ -Brass Oil-Based Nanofluid. *Metall. Mater. Trans. A* **2016**, *47*, 1409–1412. [[CrossRef](#)]
39. Xue, Q.Z. Model for effective thermal conductivity of nanofluids. *Phys. Lett. Sect. A Gen. At. Solid State Phys.* **2003**, *307*, 313–317. [[CrossRef](#)]
40. Sauvard, D. Reproductive capacity of *Tomicus piniperda* L. (Col., Scolytidae): 2. Analysis of the various sister broods. *J. Appl. Entomol.* **1993**, *116*, 25–38. [[CrossRef](#)]
41. Syam Sundar, L.; Singh, M.K.; Ferro, M.C.; Sousa, A.C.M. Experimental investigation of the thermal transport properties of graphene oxide/Co₃O₄ hybrid nanofluids. *Int. Commun. Heat Mass Transf.* **2017**, *84*, 1–10. [[CrossRef](#)]
42. Rahimi, A.; Kasaeipoor, A.; Malekshah, E.H.; Kolsi, L. Experimental and numerical study on heat transfer performance of three-dimensional natural convection in an enclosure filled with DWCNTs-water nanofluid. *Powder Technol.* **2017**, *322*, 340–352. [[CrossRef](#)]
43. Jafarimoghaddam, A.; Aberoumand, S. On the evaluation of a finned annular tube in convective heat transfer performance in the presence of Ag/oil nanofluid for a constant thermal flux rate boundary condition. *Heat Transf. Res.* **2017**, *46*, 1354–1362. [[CrossRef](#)]
44. Salimi-Yasar, H.; Zeinali Heris, S.; Shanbedi, M. Influence of soluble oil-based TiO₂ nanofluid on heat transfer performance of cutting fluid. *Tribol. Int.* **2017**, *112*, 147–154. [[CrossRef](#)]
45. Sokhansefat, T.; Kasaeian, A.B.; Kowsary, F. Heat transfer enhancement in parabolic trough collector tube using Al₂O₃/synthetic oil nanofluid. *Renew. Sustain. Energy Rev.* **2014**, *33*, 636–644. [[CrossRef](#)]
46. Sidik, N.A.C.; Adamu, I.M.; Jamil, M.M.; Kefayati, G.H.R.; Mamat, R.; Najafi, G. Recent progress on hybrid nanofluids in heat transfer applications: A comprehensive review. *Int. Commun. Heat Mass Transf.* **2016**, *78*, 68–79. [[CrossRef](#)]
47. Che Sidik, N.A.; Mahmud Jamil, M.; Aziz Japar, W.M.A.; Muhammad Adamu, I. A review on preparation methods, stability and applications of hybrid nanofluids. *Renew. Sustain. Energy Rev.* **2017**, *80*, 1112–1122. [[CrossRef](#)]
48. Manojkumar, K.; Ghosh, A. Assessment of cooling-lubrication and wettability characteristics of nano-engineered sunflower oil as cutting fluid and its impact on SQCL grinding performance. *J. Mater. Process. Technol.* **2016**, *237*, 55–64. [[CrossRef](#)]

49. Hemmat Esfe, M.; Rahimi Raki, H.; Sarmasti Emami, M.R.; Afrand, M. Viscosity and rheological properties of antifreeze based nanofluid containing hybrid nano-powders of MWCNTs and TiO₂ under different temperature conditions. *Powder Technol.* **2019**, *342*, 808–816. [[CrossRef](#)]
50. Amiri, A.; Shanbedi, M.; Ahmadi, G.; Rozali, S. Transformer oils-based graphene quantum dots nanofluid as a new generation of highly conductive and stable coolant. *Int. Commun. Heat Mass Transf.* **2017**, *83*, 40–47. [[CrossRef](#)]
51. Aghaei, A.; Khorasanizadeh, H.; Sheikhzadeh, G.A. Measurement of the dynamic viscosity of hybrid engine oil -CuO-MWCNT nanofluid, development of a practical viscosity correlation and utilizing the artificial neural network. *Heat Mass Transf.* **2018**, *54*, 151–161. [[CrossRef](#)]
52. Ilyas, S.U.; Pendyala, R.; Narahari, M.; Susin, L. Stability, rheology and thermal analysis of functionalized alumina- thermal oil-based nanofluids for advanced cooling systems. *Energy Convers. Manag.* **2017**, *142*, 215–229. [[CrossRef](#)]
53. Ilyas, S.U.; Pendyala, R.; Narahari, M. Stability and thermal analysis of MWCNT-thermal oil-based nanofluids. *Colloids Surfaces A Physicochem. Eng. Asp.* **2017**, *527*, 11–22. [[CrossRef](#)]
54. Tabora, E.A.; Alvarado, V.; Cortés, F.B. Effect of SiO₂-based nanofluids in the reduction of naphtha consumption for heavy and extra-heavy oils transport: Economic impacts on the Colombian market. *Energy Convers. Manag.* **2017**, *148*, 30–42. [[CrossRef](#)]
55. Wei, B.; Li, Q.; Ning, J.; Wang, Y.; Sun, L.; Pu, W. Macro- and micro-scale observations of a surface-functionalized nanocellulose based aqueous nanofluids in chemical enhanced oil recovery (C-EOR). *Fuel* **2019**, *236*, 1321–1333. [[CrossRef](#)]
56. Sheikholeslami, M.; Gerdroodbary, M.B.; Moradi, R.; Shafee, A.; Li, Z. Application of Neural Network for estimation of heat transfer treatment of Al₂O₃-H₂O nanofluid through a channel. *Comput. Methods Appl. Mech. Eng.* **2019**, *344*, 1–12. [[CrossRef](#)]
57. Zareh-Desari, B.; Davoodi, B. Assessing the lubrication performance of vegetable oil-based nano-lubricants for environmentally conscious metal forming processes. *J. Clean. Prod.* **2016**, *135*, 1198–1209. [[CrossRef](#)]
58. Qin, J.-H.; Liu, Z.-Q.; Li, N.; Chen, Y.-B.; Wang, D.-Y. A facile way to prepare CuS-oil nanofluids with enhanced thermal conductivity and appropriate viscosity. *J. Nanoparticle Res.* **2017**, *19*, 40. [[CrossRef](#)]
59. Zheng, C.; Cheng, Y.; Wei, Q.; Li, X.; Zhang, Z. Suspension of surface-modified nano-SiO₂ in partially hydrolyzed aqueous solution of polyacrylamide for enhanced oil recovery. *Colloids Surfaces A Physicochem. Eng. Asp.* **2017**, *524*, 169–177. [[CrossRef](#)]
60. Tabari, Z.T.; Heris, S.Z. Heat Transfer Performance of Milk Pasteurization Plate Heat Exchangers Using MWCNT/Water Nanofluid. *J. Dispers. Sci. Technol.* **2015**, *36*, 196–204. [[CrossRef](#)]
61. Saeedinia, M.; Akhavan-Behabadi, M.A.; Razi, P. Thermal and rheological characteristics of CuO-Base oil nanofluid flow inside a circular tube. *Int. Commun. Heat Mass Transf.* **2012**, *39*, 152–159. [[CrossRef](#)]
62. Moraveji, M.K.; Hejazian, M. CFD Examination of Convective Heat Transfer and Pressure Drop in a Horizontal Helically Coiled Tube with CuO/Oil Base Nanofluid. *Numer. Heat Transf. Part A Appl.* **2014**, *66*, 315–329. [[CrossRef](#)]
63. Heris, S.Z.; Farzin, F.; Sardarabadi, H. Experimental Comparison Among Thermal Characteristics of Three Metal Oxide Nanoparticles/Turbine Oil-Based Nanofluids Under Laminar Flow Regime. *Int. J. Thermophys.* **2015**, *36*, 760–782. [[CrossRef](#)]
64. Ghazvini, M.; Akhavan-Behabadi, M.A.; Rasouli, E.; Raisee, M. Heat Transfer Properties of Nanodiamond-Engine Oil Nanofluid in Laminar Flow. *Heat Transf. Eng.* **2012**, *33*, 525–532. [[CrossRef](#)]
65. Sundar, L.S.; Shusmitha, K.; Singh, M.K.; Sousa, A.C.M. Electrical conductivity enhancement of nanodiamond-nickel (ND-Ni) nanocomposite based magnetic nanofluids. *Int. Commun. Heat Mass Transf.* **2014**, *57*, 1–7. [[CrossRef](#)]
66. Ingole, S.; Charanpahari, A.; Kakade, A.; Umare, S.S.; Bhatt, D.V.; Menghani, J. Tribological behavior of nano TiO₂ as an additive in base oil. *Wear* **2013**, *301*, 776–785. [[CrossRef](#)]
67. Beheshti, A.; Shanbedi, M.; Heris, S.Z. Heat transfer and rheological properties of transformer oil-oxidized MWCNT nanofluid. *J. Therm. Anal. Calorim.* **2014**, *118*, 1451–1460. [[CrossRef](#)]
68. Abbasian Arani, A.A.; Aberoumand, H.; Aberoumand, S.; Jafari Moghaddam, A.; Dastanian, M. An empirical investigation on thermal characteristics and pressure drop of Ag-oil nanofluid in concentric annular tube. *Heat Mass Transf.* **2016**, *52*, 1693–1706. [[CrossRef](#)]
69. Wang, C.; Meng, R.; Xiao, F.; Wang, R. Use of nanoemulsion for effective removal of both oil-based drilling fluid and filter cake. *J. Nat. Gas Sci. Eng.* **2016**, *36*, 328–338. [[CrossRef](#)]
70. Su, Y.; Gong, L.; Li, B.; Liu, Z.; Chen, D. Performance evaluation of nanofluid MQL with vegetable-based oil and ester oil as base fluids in turning. *Int. J. Adv. Manuf. Technol.* **2016**, *83*, 2083–2089. [[CrossRef](#)]
71. Derakhshan, M.M.; Akhavan-Behabadi, M.A. Mixed convection of MWCNT-heat transfer oil nanofluid inside inclined plain and microfin tubes under laminar assisted flow. *Int. J. Therm. Sci.* **2016**, *99*, 1–8. [[CrossRef](#)]
72. Dardan, E.; Afrand, M.; Meghdadi Isfahani, A.H. Effect of suspending hybrid nano-additives on rheological behavior of engine oil and pumping power. *Appl. Therm. Eng.* **2016**, *109*, 524–534. [[CrossRef](#)]
73. Aberoumand, S.; Jafarimoghaddam, A.; Aberoumand, H.; Javaherdeh, K. A Complete Experimental Investigation on The Rheological Behavior of Silver Oil Based Nanofluid. *Heat Transf. Res.* **2017**, *46*, 294–304. [[CrossRef](#)]
74. Wang, P.; Liang, R.; Wang, Y.; Yu, Y.; Zhang, J.; Liu, M. The numerical investigation of heat transfer enhancement of copper-oil and diamond-oil nanofluids inside the piston cooling gallery. *Powder Technol.* **2017**, *320*, 313–324. [[CrossRef](#)]
75. Gholami, M.R.; Akbari, O.A.; Marzban, A.; Toghraie, D.; Shabani, G.A.S.; Zarringhalam, M. The effect of rib shape on the behavior of laminar flow of oil/MWCNT nanofluid in a rectangular microchannel. *J. Therm. Anal. Calorim.* **2018**, *134*, 1611–1628. [[CrossRef](#)]
76. Mechiri, S.K.; Vasu, V.; Gopal, A.V. Investigation of thermal conductivity and rheological properties of vegetable oil based hybrid nanofluids containing Cu-Zn hybrid nanoparticles. *Exp. Heat Transf.* **2017**, *30*, 205–217. [[CrossRef](#)]

77. Asadi, A.; Asadi, M.; Rezaniakolaei, A.; Rosendahl, L.A.; Wongwises, S. An experimental and theoretical investigation on heat transfer capability of Mg (OH)₂/MWCNT-engine oil hybrid nano-lubricant adopted as a coolant and lubricant fluid. *Appl. Therm. Eng.* **2018**, *129*, 577–586. [[CrossRef](#)]
78. Suleimanov, B.A.; Ismailov, F.S.; Veliyev, E.F. Nanofluid for enhanced oil recovery. *J. Pet. Sci. Eng.* **2011**, *78*, 431–437. [[CrossRef](#)]
79. Radnia, H.; Rashidi, A.; Solaimany Nazar, A.R.; Eskandari, M.M.; Jalilian, M. A novel nanofluid based on sulfonated graphene for enhanced oil recovery. *J. Mol. Liq.* **2018**, *271*, 795–806. [[CrossRef](#)]
80. Kuang, W.; Saraji, S.; Piri, M. A systematic experimental investigation on the synergistic effects of aqueous nanofluids on interfacial properties and their implications for enhanced oil recovery. *Fuel* **2018**, *220*, 849–870. [[CrossRef](#)]
81. Emadi, S.; Shadzadeh, S.R.; Manshad, A.K.; Rahimi, A.M.; Mohammadi, A.H. Effect of nano silica particles on Interfacial Tension (IFT) and mobility control of natural surfactant (Cedr Extraction) solution in enhanced oil recovery process with nano-surfactant flooding. *J. Mol. Liq.* **2017**, *248*, 163–167. [[CrossRef](#)]
82. Hemmat Esfe, M.; Rostamian, H.; Rejvani, M.; Emami, M.R.S. Rheological behavior characteristics of ZrO₂-MWCNT/10w40 hybrid nano-lubricant affected by temperature, concentration, and shear rate: An experimental study and a neural network simulating. *Phys. E Low-Dimensional Syst. Nanostructures* **2018**, *102*, 160–170. [[CrossRef](#)]
83. Dai, C.; Sun, X.; Sun, Y.; Zhao, M.; Du, M.; Zou, C.; Guan, B. The effect of supercritical CO₂ fracturing fluid retention-induced permeability alteration of tight oil reservoir. *J. Pet. Sci. Eng.* **2018**, *171*, 1123–1132. [[CrossRef](#)]
84. Liang, T.; Li, Q.; Liang, X.; Yao, E.; Wang, Y.; Li, Y.; Chen, M.; Zhou, F.; Lu, J. Evaluation of liquid nanofluid as fracturing fluid additive on enhanced oil recovery from low-permeability reservoirs. *J. Pet. Sci. Eng.* **2018**, *168*, 390–399. [[CrossRef](#)]
85. Chen, X.; Xie, X.; Li, Y.; Chen, S. Investigation of the synergistic effect of alumina nanofluids and surfactant on oil recovery—Interfacial tension, emulsion stability and viscosity reduction of heavy oil. *Pet. Sci. Technol.* **2018**, *36*, 1131–1136. [[CrossRef](#)]
86. Alnarabiji, M.S.; Yahya, N.; Nadeem, S.; Adil, M.; Baig, M.K.; Ben Ghanem, O.; Azizi, K.; Ahmed, S.; Maulianda, B.; Klemeš, J.J.; et al. Nanofluid enhanced oil recovery using induced ZnO nanocrystals by electromagnetic energy: Viscosity increment. *Fuel* **2018**, *233*, 632–643. [[CrossRef](#)]
87. Al-Anssari, S.; Arif, M.; Wang, S.; Barifcani, A.; Lebedev, M.; Iglauer, S. Wettability of nanofluid-modified oil-wet calcite at reservoir conditions. *Fuel* **2018**, *211*, 405–414. [[CrossRef](#)]
88. Zabala, R.; Franco, C.A.; Cortés, F.B. Application of Nanofluids for Improving Oil Mobility in Heavy Oil and Extra-Heavy Oil: A Field Test. In Proceedings of the SPE Improved Oil Recovery Conference, Tulsa, OK, USA, 11–13 April 2016.
89. Shahrabadi, A.; Bagherzadeh, H.; Roostaie, A.; Golghanddashti, H. Experimental Investigation of HLP Nanofluid Potential to Enhance Oil Recovery: A Mechanistic Approach. In Proceedings of the SPE International Oilfield Nanotechnology Conference and Exhibition, Noordwijk, The Netherlands, 12–14 June 2012.
90. Hendraningrat, L.; Torsæter, O. Metal oxide-based nanoparticles: Revealing their potential to enhance oil recovery in different wettability systems. *Appl. Nanosci.* **2015**, *5*, 181–199. [[CrossRef](#)]
91. Zhao, K.; Li, D. Manipulation and separation of oil droplets by using asymmetric nano-orifice induced DC dielectrophoretic method. *J. Colloid Interface Sci.* **2018**, *512*, 389–397. [[CrossRef](#)]
92. Youssif, M.I.; El-Maghraby, R.M.; Saleh, S.M.; Elgibaly, A. Silica nanofluid flooding for enhanced oil recovery in sandstone rocks. *Egypt. J. Pet.* **2018**, *27*, 105–110. [[CrossRef](#)]
93. Bhunia, M.M.; Panigrahi, K.; Das, S.; Chattopadhyay, K.K.; Chattopadhyay, P. Amorphous graphene—Transformer oil nanofluids with superior thermal and insulating properties. *Carbon N. Y.* **2018**, *139*, 1010–1019. [[CrossRef](#)]
94. Rubalya Valantina, S.; Arockia Jayalatha, K.; Phebee Angeline, D.R.; Uma, S.; Ashvanth, B. Synthesis and characterisation of electro-rheological property of novel eco-friendly rice bran oil and nanofluid. *J. Mol. Liq.* **2018**, *256*, 256–266. [[CrossRef](#)]
95. Gbadamosi, A.O.; Junin, R.; Manan, M.A.; Yekeen, N.; Agi, A.; Oseh, J.O. Recent advances and prospects in polymeric nanofluids application for enhanced oil recovery. *J. Ind. Eng. Chem.* **2018**, *66*, 1–19. [[CrossRef](#)]
96. Fontes, D.H.; Ribatski, G.; Bandarra Filho, E.P. Experimental evaluation of thermal conductivity, viscosity and breakdown voltage AC of nanofluids of carbon nanotubes and diamond in transformer oil. *Diam. Relat. Mater.* **2015**, *58*, 115–121. [[CrossRef](#)]
97. Khademolhosseini, R.; Jafari, A.; Shabani, M.H. Micro Scale Investigation of Enhanced Oil Recovery Using Nano/Bio Materials. *Procedia Mater. Sci.* **2015**, *11*, 171–175. [[CrossRef](#)]
98. Murshed, S.M.S.; Tan, S.H.; Nguyen, N.T. Temperature dependence of interfacial properties and viscosity of nanofluids for droplet-based microfluidics. *J. Phys. D. Appl. Phys.* **2008**, *41*, 085502. [[CrossRef](#)]
99. Mohammadi, M.; Dadvar, M.; Dabir, B. Application of response surface methodology for optimization of the stability of asphaltene particles in crude oil by TiO₂/SiO₂ nanofluids under static and dynamic conditions. *J. Dispers. Sci. Technol.* **2018**, *39*, 431–442. [[CrossRef](#)]
100. Hussein, A.M.; Lingenthiran; Kadirgama, K.; Noor, M.M.; Aik, L.K. Palm oil based nanofluids for enhancing heat transfer and rheological properties. *Heat Mass Transf.* **2018**, *54*, 3163–3169. [[CrossRef](#)]
101. Liu, H.; Yu, Y.; Liu, H.; Jin, J.; Liu, S. Hybrid effects of nano-silica and graphene oxide on mechanical properties and hydration products of oil well cement. *Constr. Build. Mater.* **2018**, *191*, 311–319. [[CrossRef](#)]
102. Qi, C.; Liu, M.; Wang, G.; Pan, Y.; Liang, L. Experimental research on stabilities, thermophysical properties and heat transfer enhancement of nanofluids in heat exchanger systems. *Chinese J. Chem. Eng.* **2018**, *26*, 2420–2430. [[CrossRef](#)]

103. Lee, P.H.; Nam, J.S.; Li, C.; Lee, S.W. An experimental study on micro-grinding process with nanofluid minimum quantity lubrication (MQL). *Int. J. Precis. Eng. Manuf.* **2012**, *13*, 331–338. [[CrossRef](#)]
104. Razi, P.; Akhavan-Behabadi, M.A.; Saedinia, M. Pressure drop and thermal characteristics of CuO–base oil nanofluid laminar flow in flattened tubes under constant heat flux. *Int. Commun. Heat Mass Transf.* **2011**, *38*, 964–971. [[CrossRef](#)]
105. Ariana, M.A.; Vaferi, B.; Karimi, G. Prediction of thermal conductivity of alumina water-based nanofluids by artificial neural networks. *Powder Technol.* **2015**, *278*, 1–10. [[CrossRef](#)]
106. Ragavan, G.; Muralidaran, Y.; Sridharan, B.; Nachiappa Ganesh, R.; Viswanathan, P. Evaluation of garlic oil in nano-emulsified form: Optimization and its efficacy in high-fat diet induced dyslipidemia in Wistar rats. *Food Chem. Toxicol.* **2017**, *105*, 203–213. [[CrossRef](#)] [[PubMed](#)]
107. Gao, H.; Yang, H.; Wang, C. Controllable preparation and mechanism of nano-silver mediated by the microemulsion system of the clove oil. *Results Phys.* **2017**, *7*, 3130–3136. [[CrossRef](#)]
108. Hazer, B.; Kalaycı, Ö.A. High fluorescence emission silver nano particles coated with poly (styrene-g-soybean oil) graft copolymers: Antibacterial activity and polymerization kinetics. *Mater. Sci. Eng. C* **2017**, *74*, 259–269. [[CrossRef](#)]
109. Subramanian, S.; Devadasan Racheal, P.A.; Sathianathan, R.V.; Rajagopal, A. Structural and Dielectric Properties of Groundnut Oil, Mustard Oil and ZnO Nanofluid. *Iran. J. Sci. Technol. Trans. A Sci.* **2019**, *43*, 1351–1359. [[CrossRef](#)]
110. Gao, T.; Li, C.; Zhang, Y.; Yang, M.; Jia, D.; Jin, T.; Hou, Y.; Li, R. Dispersing mechanism and tribological performance of vegetable oil-based CNT nanofluids with different surfactants. *Tribol. Int.* **2019**, *131*, 51–63. [[CrossRef](#)]
111. Jafarimoghaddam, A.; Aberoumand, S.; Javaherdeh, K.; Arani, A.A.A.; Jafarimoghaddam, R. Al/oil nanofluids inside annular tube: An experimental study on convective heat transfer and pressure drop. *Heat Mass Transf.* **2018**, *54*, 1053–1067. [[CrossRef](#)]
112. Yuan, S.; Hou, X.; Wang, L.; Chen, B. Experimental Investigation on the Compatibility of Nanoparticles with Vegetable Oils for Nanofluid Minimum Quantity Lubrication Machining. *Tribol. Lett.* **2018**, *66*, 106. [[CrossRef](#)]
113. Adenutsi, C.D.; Li, Z.; Aggrey, W.N.; Toro, B.L. Performance of Relative Permeability and Two-Phase Flow Parameters Under Net Effective Stress in Water Wet Porous Media: A Comparative Study of Water–Oil Versus Silica Nanofluid–Oil. *Arab. J. Sci. Eng.* **2018**, *43*, 6555–6565. [[CrossRef](#)]
114. Wang, Y.; Li, C.; Zhang, Y.; Yang, M.; Li, B.; Dong, L.; Wang, J. Processing Characteristics of Vegetable Oil-based Nanofluid MQL for Grinding Different Workpiece Materials. *Int. J. Precis. Eng. Manuf. Technol.* **2018**, *5*, 327–339. [[CrossRef](#)]
115. Wang, X.; He, Y.; Chen, M.; Hu, Y. Solar Energy Materials and Solar Cells ZnO-Au composite hierarchical particles dispersed oil-based nano fluids for direct absorption solar collectors. *Sol. Energy Mater. Sol. Cells* **2018**, *179*, 185–193. [[CrossRef](#)]
116. Shen, L.P.; Wang, H.; Dong, M.; Ma, Z.C.; Wang, H.B. Solvothermal synthesis and electrical conductivity model for the zinc oxide-insulated oil nanofluid. *Phys. Lett. A* **2012**, *376*, 1053–1057. [[CrossRef](#)]
117. Al-Nimr, M.A.; Al-Dafaie, A.M.A. Using nanofluids in enhancing the performance of a novel two-layer solar pond. *Energy* **2014**, *68*, 318–326. [[CrossRef](#)]
118. Khakrah, H.; Shamloo, A.; Kazemzadeh Hannani, S. Exergy analysis of parabolic trough solar collectors using Al₂O₃/synthetic oil nanofluid. *Sol. Energy* **2018**, *173*, 1236–1247. [[CrossRef](#)]
119. Gulzar, O.; Qayoum, A.; Gupta, R. Photo-thermal characteristics of hybrid nanofluids based on Therminol-55 oil for concentrating solar collectors. *Appl. Nanosci.* **2018**, *9*, 1133–1143. [[CrossRef](#)]
120. Wang, Y.; Xu, J.; Liu, Q.; Chen, Y.; Liu, H. Performance analysis of a parabolic trough solar collector using Al₂O₃/synthetic oil nanofluid. *Appl. Therm. Eng.* **2016**, *107*, 469–478. [[CrossRef](#)]
121. Loni, R.; Asli-Ardeh, E.A.; Ghobadian, B.; Ahmadi, M.H.; Bellos, E. GMDH modeling and experimental investigation of thermal performance enhancement of hemispherical cavity receiver using MWCNT/oil nanofluid. *Sol. Energy* **2018**, *171*, 790–803. [[CrossRef](#)]
122. Hendraningrat, L.; Li, S.; Torsæter, O. A coreflood investigation of nanofluid enhanced oil recovery. *J. Pet. Sci. Eng.* **2013**, *111*, 128–138. [[CrossRef](#)]
123. Zhang, H.; Nikolov, A.; Wasan, D. Enhanced Oil Recovery (EOR) Using Nanoparticle Dispersions: Underlying Mechanism and Imbibition Experiments. *Energy Fuels* **2014**, *28*, 3002–3009. [[CrossRef](#)]
124. Alomair, O.A.; Matar, K.M.; Alsaeed, Y.H. Nanofluids Application for Heavy Oil Recovery. In Proceedings of the SPE Asia Pacific Oil and Gas Conference and Exhibition, Adelaide, Australia, 14–15 October 2014. [[CrossRef](#)]
125. Lee, J.; Babadagli, T. Comprehensive methodology for chemicals and nano materials screening for heavy oil recovery using microemulsion characterization. *J. Pet. Sci. Eng.* **2018**, *171*, 1099–1112. [[CrossRef](#)]
126. Li, B.; Li, C.; Zhang, Y.; Wang, Y.; Yang, M.; Jia, D.; Zhang, N.; Wu, Q. Effect of the physical properties of different vegetable oil-based nanofluids on MQLC grinding temperature of Ni-based alloy. *Int. J. Adv. Manuf. Technol.* **2017**, *89*, 3459–3474. [[CrossRef](#)]
127. Padmini, R.; Vamsi Krishna, P.; Krishna Mohana Rao, G. Effectiveness of vegetable oil based nanofluids as potential cutting fluids in turning AISI 1040 steel. *Tribol. Int.* **2016**, *94*, 490–501. [[CrossRef](#)]
128. Li, M.; Yu, T.; Yang, L.; Li, H.; Zhang, R.; Wang, W. Parameter optimization during minimum quantity lubrication milling of TC4 alloy with graphene-dispersed vegetable-oil-based cutting fluid. *J. Clean. Prod.* **2019**, *209*, 1508–1522. [[CrossRef](#)]
129. Rapeti, P.; Pasam, V.K.; Rao Gurram, K.M.; Revuru, R.S. Performance evaluation of vegetable oil based nano cutting fluids in machining using grey relational analysis-A step towards sustainable manufacturing. *J. Clean. Prod.* **2018**, *172*, 2862–2875. [[CrossRef](#)]

130. Lv, Y.Z.; Wang, J.; Yi, K.; Wang, W.; Li, C. Effect of Oleic Acid Surface Modification on Dispersion Stability and Breakdown Strength of Vegetable Oil-Based Fe₃O₄ Nanofluids. *Integr. Ferroelectr.* **2015**, *163*, 21–28. [[CrossRef](#)]
131. Jiang, W.; Ding, G.; Peng, H.; Hu, H. Modeling of nanoparticles' aggregation and sedimentation in nanofluid. *Curr. Appl. Phys.* **2010**, *10*, 934–941. [[CrossRef](#)]
132. Jafarimoghaddam, A.; Aberoumand, S.; Aberoumand, H.; Javaherdeh, K. Experimental Study on Cu/Oil Nanofluids through Concentric Annular Tube: A Correlation. *Heat Transf. Res.* **2017**, *46*, 251–260. [[CrossRef](#)]
133. Li, J.; Du, B.; Wang, F.; Yao, W.; Yao, S. The effect of nanoparticle surfactant polarization on trapping depth of vegetable insulating oil-based nanofluids. *Phys. Lett. A* **2016**, *380*, 604–608. [[CrossRef](#)]
134. Li, B.; Li, C.; Zhang, Y.; Wang, Y.; Jia, D.; Yang, M.; Zhang, N.; Wu, Q.; Han, Z.; Sun, K. Heat transfer performance of MQL grinding with different nanofluids for Ni-based alloys using vegetable oil. *J. Clean. Prod.* **2017**, *154*, 1–11. [[CrossRef](#)]
135. Mohammad, R.; Kandasamy, R. Nanoparticle shapes on electric and magnetic force in water, ethylene glycol and engine oil based Cu, Al₂O₃ and SWCNTs. *J. Mol. Liq.* **2017**, *237*, 54–64. [[CrossRef](#)]
136. Ur Rehman, A.; Mehmood, R.; Nadeem, S.; Akbar, N.S.; Motsa, S.S. Effects of single and multi-walled carbon nano tubes on water and engine oil based rotating fluids with internal heating. *Adv. Powder Technol.* **2017**, *28*, 1991–2002. [[CrossRef](#)]
137. Tao, P.; Shu, L.; Zhang, J.; Lee, C.; Ye, Q.; Guo, H.; Deng, T. Silicone oil-based solar-thermal fluids dispersed with PDMS-modified Fe₃O₄@graphene hybrid nanoparticles. *Prog. Nat. Sci. Mater. Int.* **2018**, *28*, 554–562. [[CrossRef](#)]
138. Asadi, M.; Asadi, A.; Aberoumand, S. An experimental and theoretical investigation on the effects of adding hybrid nanoparticles on heat transfer efficiency and pumping power of an oil-based nanofluid as a coolant fluid. *Int. J. Refrig.* **2018**, *89*, 83–92. [[CrossRef](#)]
139. Pryazhnikov, M.I.; Minakov, A.V.; Rudyak, V.Y.; Guzei, D. V Thermal conductivity measurements of nanofluids. *Int. J. Heat Mass Transf.* **2017**, *104*, 1275–1282. [[CrossRef](#)]
140. Mashhadi, S.; Javadian, H.; Tyagi, I.; Agarwal, S.; Gupta, V.K. The effect of Na₂SO₄ concentration in aqueous phase on the phase inversion temperature of lemon oil in water nano-emulsions. *J. Mol. Liq.* **2016**, *215*, 454–460. [[CrossRef](#)]
141. Dinesh, R.; Prasad, M.J.G.; Kumar, R.R.; Santharaj, N.J.; Santhip, J.; Raaj, A.S.A. Investigation of Tribological and Thermophysical Properties of Engine Oil Containing Nano additives. *Mater. Today Proc.* **2016**, *3*, 45–53. [[CrossRef](#)]
142. He, C.; Ding, Y.; Chen, J.; Wang, F.; Gao, C.; Zhang, S.; Yang, M. Influence of the nano-hybrid pour point depressant on flow properties of waxy crude oil. *Fuel* **2016**, *167*, 40–48. [[CrossRef](#)]
143. Quercia, G.; Brouwers, H.J.H.; Garnier, A.; Luke, K. Influence of olivine nano-silica on hydration and performance of oil-well cement slurries. *Mater. Des.* **2016**, *96*, 162–170. [[CrossRef](#)]
144. Sgroi, M.F.; Asti, M.; Gili, F.; Deorsola, F.A.; Bensaid, S.; Fino, D.; Kraft, G.; Garcia, I.; Dassenoy, F. Engine bench and road testing of an engine oil containing MoS₂ particles as nano-additive for friction reduction. *Tribol. Int.* **2017**, *105*, 317–325. [[CrossRef](#)]
145. Asadi, A.; Pourfattah, F. Heat transfer performance of two oil-based nanofluids containing ZnO and MgO nanoparticles; a comparative experimental investigation. *Powder Technol.* **2019**, *343*, 296–308. [[CrossRef](#)]
146. Gara, L.; Zou, Q. Friction and Wear Characteristics of Oil-Based ZnO Nanofluids. *Tribol. Trans.* **2013**, *56*, 236–244. [[CrossRef](#)]
147. Fontes, D.H.; Padilla, E.L.M.; dos Santos, D.D.; Bandarra Filho, E.P. Numerical study of the natural convection of nanofluids based on mineral oil with properties evaluated experimentally. *Int. Commun. Heat Mass Transf.* **2017**, *85*, 107–113. [[CrossRef](#)]
148. Hameed, A.; Mukhtar, A.; Shafiq, U.; Qizilbash, M.; Khan, M.S.; Rashid, T.; Bavoh, C.B.; Rehman, W.U.; Guardo, A. Experimental investigation on synthesis, characterization, stability, thermo-physical properties and rheological behavior of MWCNTs-kapok seed oil based nanofluid. *J. Mol. Liq.* **2019**, *277*, 812–824. [[CrossRef](#)]
149. Lv, Y.; Li, C.; Sun, Q.; Huang, M.; Li, C.; Qi, B. Effect of Dispersion Method on Stability and Dielectric Strength of Transformer Oil-Based TiO₂ Nanofluids. *Nanoscale Res. Lett.* **2016**, *11*, 515. [[CrossRef](#)] [[PubMed](#)]
150. Asadi, A.; Asadi, M.; Rezaniakolaei, A.; Rosendahl, L.A.; Afrand, M.; Wongwises, S. Heat transfer efficiency of Al₂O₃-MWCNT/thermal oil hybrid nanofluid as a cooling fluid in thermal and energy management applications: An experimental and theoretical investigation. *Int. J. Heat Mass Transf.* **2018**, *117*, 474–486. [[CrossRef](#)]
151. Loni, R.; Askari Asli-ardeh, E.; Ghobadian, B.; Kasaeian, A.B.; Gorjian, S. Thermodynamic analysis of a solar dish receiver using different nanofluids. *Energy* **2017**, *133*, 749–760. [[CrossRef](#)]
152. Loni, R.; Askari Asli-Ardeh, E.; Ghobadian, B.; Kasaeian, A.B.; Bellos, E. Thermal performance comparison between Al₂O₃/oil and SiO₂/oil nanofluids in cylindrical cavity receiver based on experimental study. *Renew. Energy* **2018**, *129*, 652–665. [[CrossRef](#)]
153. Loni, R.; Asli-Ardeh, E.A.; Ghobadian, B.; Kasaeian, A. Experimental study of carbon nano tube/oil nanofluid in dish concentrator using a cylindrical cavity receiver: Outdoor tests. *Energy Convers. Manag.* **2018**, *165*, 593–601. [[CrossRef](#)]
154. Herper, H.C.; Entel, P. Influence of domain wall scattering on the magnetoresistance of Co and Co₈₀Pt₂₀ film systems. *Phys. Rev. B -Condens. Matter Mater. Phys.* **2008**, *77*, 174406. [[CrossRef](#)]
155. Mohammadi, A.; Jafari, S.M.; Esfanjani, A.F.; Akhavan, S. Application of nano-encapsulated olive leaf extract in controlling the oxidative stability of soybean oil. *Food Chem.* **2016**, *190*, 513–519. [[CrossRef](#)]
156. Loni, R.; Asli-Ardeh, E.A.; Ghobadian, B.; Kasaeian, A.B.; Bellos, E. Energy and exergy investigation of alumina/oil and silica/oil nanofluids in hemispherical cavity receiver: Experimental Study. *Energy* **2018**, *164*, 275–287. [[CrossRef](#)]